Quarterly Progress Report

September 1, 1996 to November 29, 1996

Visible Light Emitting Materials and Injection Devices

ONR/DARPA URI

Grant Number N00014-92-J-1895

Prepared by:

Paul H. Holloway
Department of Materials Science and Engineering
University of Florida
P.O. Box 116400
Gainesville, FL 32611
Ph: 352/392-6664; FAX: 352/392-4911
E-Mail: Internet - pholl@silica.mse.ufl.edu

Participants:
University of Florida
Kevin Jones
Robert Park
Joseph Simmons
Cammy Abernathy
Stephen Pearton
Dept. Materials Science and Engineering
Timothy Anderson
Dept. of Chemical Engineering
Peter Zory
Dept. of Electrical Engineering
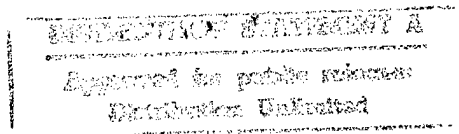**Columbia University**
Gertrude Neumark
Dept. of Materials Science and Engineering
Oregon Graduate Institute of Science and Engineering
Reinhart Engelmann
Dept. of Electrical Engineering

REPORT DOCUMENTATION PAGE

FORM APPROVED
OMB No. 0704-0188

1. AGENCY USE ONLY (Leave blank)	2. REPORT DATE	3. REPORT TYPE AND DATES COVERED
	January 15, 1997	Quarter -- Sept. 1, 1996 to Nov. 29, 1996

4. TITLE AND SUBTITLE OF REPORT

Visible Light Emitting Materials and Injection Devices

5. FUNDING NUMBERS

ONR Grant
N00014-92-J-1895

6. AUTHOR(S)

Paul H. Holloway

7. PERFORMING ORGANIZATION NAME(S) AND ADDRESS(ES)

Department of Materials Science and ENgineering
University of Florida
P.O. Box 116400
Gainesville, FL 32611-6400

8. PERFORMING ORGANIZATION REPORT NUMBER:

N/A

9. SPONSORING/MONITORING AGENCY NAME(S) AND ADDRESS(ES)

Office of Naval Research
800 North Quincy Street
Arlington, VA 22217-5000

10. SPONSORING/MONITORING AGENCY REPORT NUMBER:

11. SUPPLEMENTARY NOTES:

12a. DISTRIBUTION AVAILABILITY STATEMENT

Unlimited

12b. DISTRIBUTION CODE

13. ABSTRACT (Maximum 200 words)

Progress in report on research into ZnSe-based and GaN-based materials and devices for light emitting diodes and diode lasers at blue-green visible wavelengths.

14. SUBJECT TERMS

Zinc Selenide	Diode Lasers
Gallium Nitride	
Light Emitting Diodes	

15. NUMBER OF PAGES:
33

16. PRICE CODE

17. SECURITY CLASSIFICATION OF REPORT:	18. SECURITY CLASSIFICATION OF THIS PAGE	19. SECURITY CLASSIFICATION OF ABSTRACT	20. LIMITATION OF ABSTRACT
None	None	None	None

GENERAL INSTRUCTIONS FOR COMPLETING SF 298

The Report Documentation Page (RDP) is used in announcing and cataloging reports. It is important that this information be consistent with the rest of the report, particularly the cover and title page. Instructions for filling in each block of the form follow. It is important to *stay within the lines* to meet *optical scanning requirements*.

Block 1. Agency Use Only (Leave blank).

Block 2. Report Date. Full publication date including day, month, and year, if available (e.g. 1 Jan 88). Must cite at least the year.

Block 3. Type of Report and Dates Covered. State whether report is interim, final, etc. If applicable, enter inclusive report dates (e.g. 10 Jun 87 - 30 Jun 88).

Block 4. Title and Subtitle. A title is taken from the part of the report that provides the most meaningful and complete information. When a report is prepared in more than one volume, repeat the primary title, add volume number, and include subtitle for the specific volume. On classified documents enter the title classification in parentheses.

Block 5. Funding Numbers. To include contract and grant numbers; may include program element number(s), project number(s), task number(s), and work unit number(s). Use the following labels:

C	- Contract	PR	- Project
G	- Grant	TA	- Task
PE	- Program Element	WU	- Work Unit Accession No.

Block 6. Author(s). Name(s) of person(s) responsible for writing the report, performing the research, or credited with the content of the report. If editor or compiler, this should follow the name(s).

Block 7. Performing Organization Name(s) and Address(es). Self-explanatory.

Block 8. Performing Organization Report Number. Enter the unique alphanumeric report number(s) assigned by the organization performing the report.

Block 9. Sponsoring/Monitoring Agency Name(s) and Address(es). Self-explanatory.

Block 10. Sponsoring/Monitoring Agency Report Number. *(If known)*

Block 11. Supplementary Notes. Enter information not included elsewhere such as: Prepared in cooperation with...; Trans. of...; To be published in.... When a report is revised, include a statement whether the new report supersedes or supplements the older report.

Block 12a. Distribution/Availability Statement. Denotes public availability or limitations. Cite any availability to the public. Enter additional limitations or special markings in all capitals (e.g. NOFORN, REL, ITAR).

DOD - See DoDD 5230.24, "Distribution Statements on Technical Documents."
DOE - See authorities.
NASA - See Handbook NHB 2200.2.
NTIS - Leave blank.

Block 12b. Distribution Code.

DOD - Leave blank.
DOE - Enter DOE distribution categories from the Standard Distribution for Unclassified Scientific and Technical Reports.
NASA - Leave blank.
NTIS - Leave blank.

Block 13. Abstract. Include a brief *(Maximum 200 words)* factual summary of the most significant information contained in the report.

Block 14. Subject Terms. Keywords or phrases identifying major subjects in the report.

Block 15. Number of Pages. Enter the total number of pages.

Block 16. Price Code. Enter appropriate price code *(NTIS only)*.

Blocks 17. - 19. Security Classifications. Self-explanatory. Enter U.S. Security Classification in accordance with U.S. Security Regulations (i.e., UNCLASSIFIED). If form contains classified information, stamp classification on the top and bottom of the page.

Block 20. Limitation of Abstract. This block must be completed to assign a limitation to the abstract. Enter either UL (unlimited) or SAR (same as report). An entry in this block is necessary if the abstract is to be limited. If blank, the abstract is assumed to be unlimited.

(I)   Growth by MBE and Characterization of GaN (Robert Park)

III-V Nitride Work

As noted in the previous report, we have observed that the optical quality of MBE-grown GaN films can be significantly improved by using an alternate element exposure technique in which Ga and N atoms are exposed to the substrate separately (as opposed to simultaneously as in conventional growth). By optical quality improvement we mean an enhancement of the near-band-edge PL emission and a reduction or elimination of the deep level (yellow band) emission. We noted, in particular, that the optical quality of GaN films was maximized by virtue of incorporating an optimum time delay (30 seconds for a substrate temperature of 600°C) between closing the Ga shutter (ending Ga exposure to the substrate) and opening the N shutter (beginning N exposure to the substrate) in each cycle of growth.

In the work reported in this quarter, an attempt was made to understand the influence of the Ga delay time (time allowed to elapse between closing the Ga shutter and opening the N shutter) on the optical qualityof the GaN films. To this end, the RHEED specular reflection beam intensity was monitored during the Ga delay phase as a function of temperature.

By performing such real-time in-situ analysis, we discovered two distinct stages of recovery with regard to the surface morphology during a Ga delay phase. The two stages of recovery are illustrated in Fig. I.1 with reference to a RHEED intensity trace recorded during one cycle of growth at a substrate temperature of 600°C.

As can be seen from Fig. I.1, the Ga exposed surface recovers quickly initially, as indicated by the first-stage of recovery phase in which the specular reflection beam intensity varies approximately linearly with time following closure of the Ga shutter. Morphological change is more sluggish in the indicated second-stage of recovery in which the intensity of the specular reflection varies non-linearly with time. The specular reflection intensity actually goes through a maximum in the second-stage of recovery which suggests that there is an optimum Ga delay with regard to surface morphology (smoothness) at a particular substrate temperature.

Our interpretation of the trace characteristics shown in Fig. I.1 is that the initial (first-stage) recovery (surface smoothing) is due to fast Ga adatom migration to step edges in the absence of N atoms impinging on the surface while in the second state further smoothing of the surface is associated with terrace rearrangement which enhances long-range order. We speculate that step-bunching might be responsible for the slight increase in surface roughness for Ga delay times in excess of the optimum time.

RHEED specular reflection beam intensity traces were recorded at a variety of substrate temperatures in the range, 560 - 640°C, and we observed that the time to completion of the first-stage of recovery was a function of temperature. In fact, as shown in Fig. I.2, an Arrhenius behavior was determined for this data. Consequently, we believe that the first-stage of recovery represents that attainment of short-range order in which Ga adatom migration occurs on the terraces and, as indicated in Fig. I.2, the activation energy for Ga adatom migration was determined to be 1.46 ± 0.25 eV in the absence of impinging N atoms. To our knowledge, this is the first report of a Ga adatom migration activation energy determination on GaN surfaces.
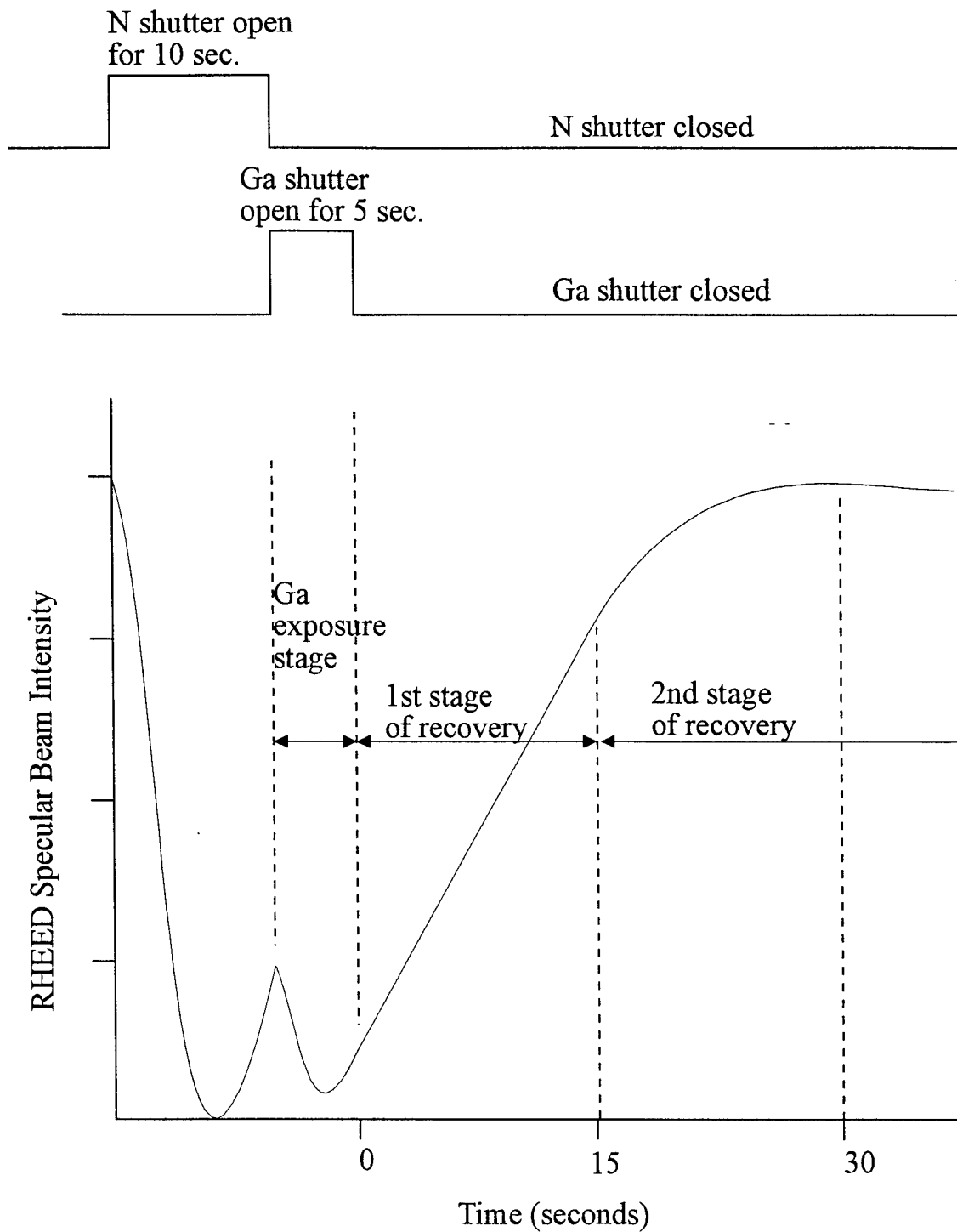
Fig. I.1. A typical trace of the RHEED specular reflection beam intensity recorded during one cycle of alternate element exposure growth of GaN with the inclusion of a Ga delay phase. In this example the substrate temperature was 600°C.
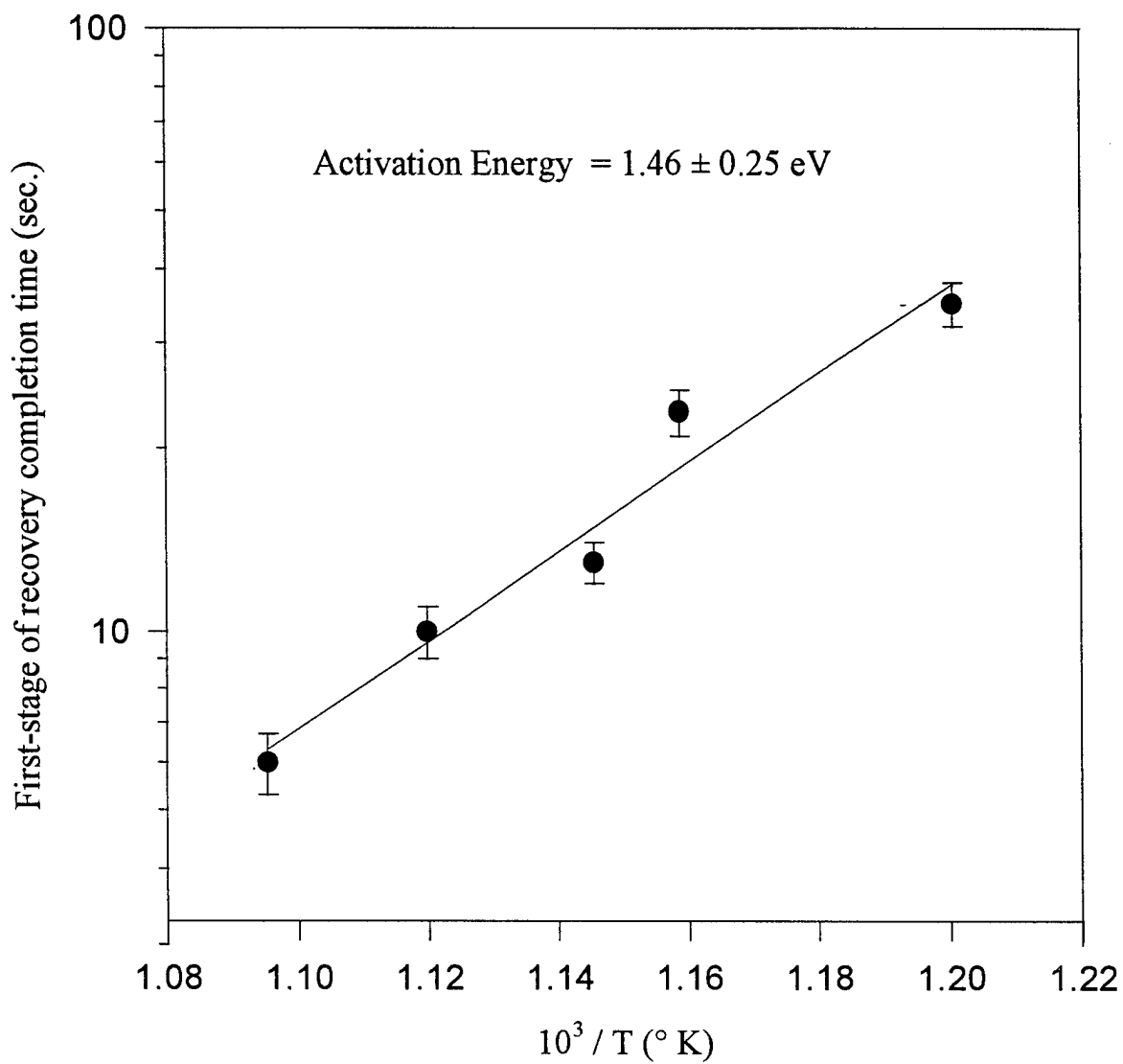
Fig. I.2. Times to complete the first-stage of recovery (attainment of short-range order through Ga adatom migration) as a function of substrate temperature in the range, 560 - 640°C

(II)   Growth and processing of GaN-based materials (Cammy Abernathy and Steve Pearton)

a.   Reactivation of acceptors and trapping of hydrogen in GaN/InGaN double heterostructures.

Hydrogen plays an important role in GaN and related alloys, since it is part of the growth environment for Metal Organic Chemical Vapor Deposition (MOCVD), which employs $(CH_3)_3Ga$ and NH_3 as its standard precursors. Hydrogen remaining in Mg-doped GaN layers has been identified as the cause of the high resistivity of these films, since it appears that the hydrogen forms stable neutral complexes $(Mg-H)^0$, with the Mg acceptors. Post-growth annealing at ~700°C, or exposure to a low energy electron beam reactivates the Mg acceptors and produces conductivities 5-6 orders of magnitude higher than in the as-grown material. Hydrogen has been shown to be injected into GaN during a number of processing steps, including dry etching in CH_4/H_2 plasma chemistries, boiling in water, wet etching in KOH solutions and chemical vapor deposition of dielectrics using SiH_4.

The behavior of hydrogen in device structures is likely to be more complicated. For example light-emitting diodes or laser diodes contain both n-and p-type GaN cladding layers with one or more InGaN active regions. The first laser diode reported by Nakamura et al. contained 26 InGaN quantum wells. In other III-V semiconductors the diffusivity of atomic hydrogen is a strong function of conductivity type and doping level since trapping by acceptors is usually more thermally stable and more efficient than trapping of hydrogen by donor impurities. Moreover hydrogen is attracted to any region of strain within multilayer structures and has been shown to pile-up at heterointerfaces in the GaAs/Si, GaAs/InP and GaAs/AlAs materials systems. Therefore it is of interest to investigate the reactivation of acceptors and trapping of hydrogen in double heterostructure GaN/InGaN samples, since these are the basis for optical emitters. We find that the reactivation of passivated Mg acceptors also depends on the annealing ambient, with an apparently higher stability for annealing under H_2 rather than N_2. Hydrogen is found to redistribute to the regions of highest defect density within the structure.

The sample was grown by MOCVD in a rotating disc reactor on c-plane Al_2O_3. The sapphire substrate was rinsed in H_2SO_4, methanol and acetone prior to loading into the growth chamber, where it was first baked at 1100°C under H_2. A low temperature (~510°C) GaN buffer (~300Å thick) was followed by 3·3μm of n$^+$ GaN (n = 10^{18}cm^{-3}, Si-doped), 0·1μm InGaN (undoped) and 0·5μm thick p$^+$GaN (p = 3X10^{17}cm^{-3}, Mg-doped). The growth temperature was 1040°C for the GaN and ~800°C for the InGaN. Cross-sectional transmission electron microscope (XTEM) analysis was carried out on the MOCVD grown InGaN/GaN double-heterostructure. An XTEM bright-field image, obtained using two-beam diffraction conditions with **g**=(2$\underline{11}$0) along the [0$\underline{11}$0]$_{GaN}$ zone axis of the DH-LED structure is shown in Fig. II.1 (left). The interface between the various layers appears to be abrupt with no indication of interfacial phases. Selected-area-diffraction (SAD) and high resolution electron microscopy revealed that the entire DH-LED structure grew epitaxially on the substrate.

In the immediate vicinity of the n-GaN/Al_2O_3 interface, the defect density was high but was reduced with increasing film thickness. However, after the growth of the active layer (InGaN) the defect density of the threading dislocations increased as shown at the right of Fig. II.1. A possible reason could be due to the different growth conditions used for growing the

p−GaN

InGaN

n−GaN

0.1 µm

p−GaN
InGaN

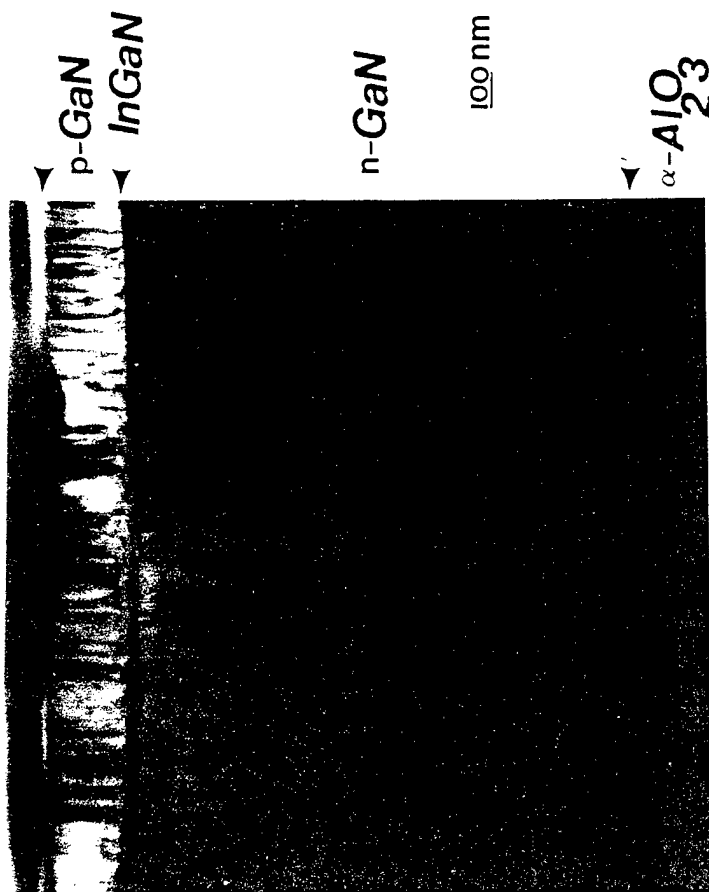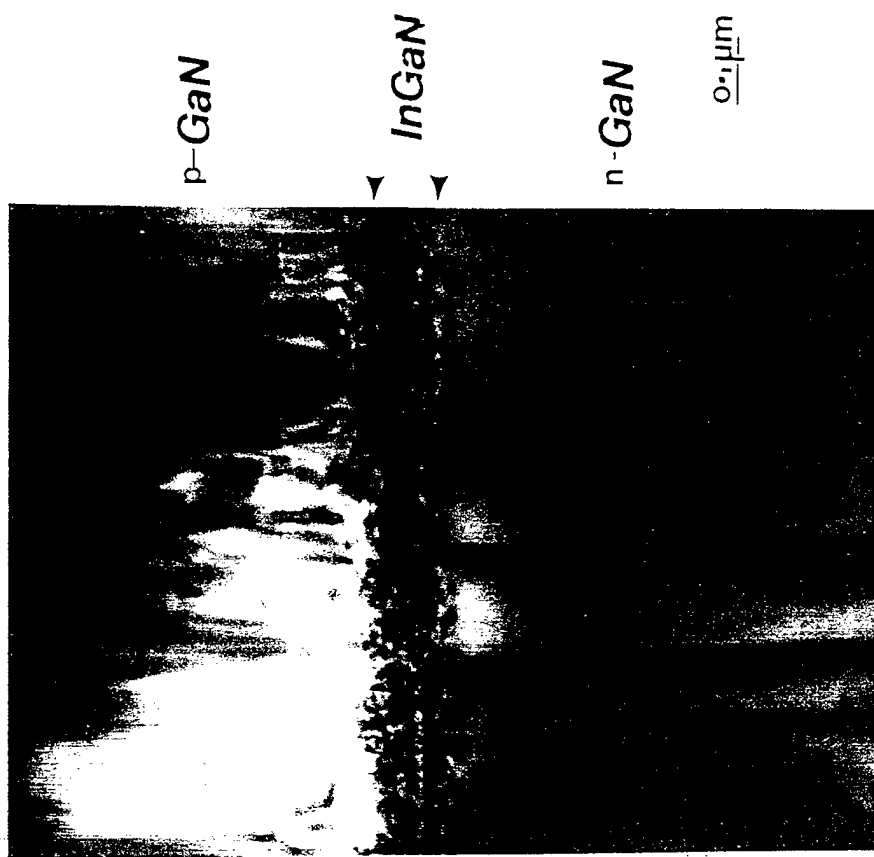n−GaN

100 nm

α−AlO$_{2}$$_{3}$

Fig. II.1.

active layer and the GaN layers. The growth mechanism for p-GaN on InGaN in the DH-LED structure could be similar to that proposed by Hiramatsu. During the growth of the subsequent p-GaN layer the underlying active layer may be undergoing solid-phase-epitaxy. Hence, the quality of p-GaN grown on top of the active layer depends on the amount of epitaxy undergone by the active layer, and in this structure the thermal degradation of the InGaN upon raising the growth temperature for the p-GaN leads to a higher defect density in this overlayer.

XTEM of the DH-LED showed dislocations as dark lines propagating in the direction normal to the substrate. Most of the dislocations appeared to traverse the entire double heterostructure, while some appeared to bend and follow the interface for a short distance before threading out to the surface. The nature of the threading dislocations was studied by conventional XTEM using the $\mathbf{g.b}$=0 criteria. The dislocation will be invisible when $\mathbf{b}$ lies in the reflecting plane.

Some of the dislocations were invisible both in $\mathbf{g2}$=(0002) and $\mathbf{g5}$=(1$\underline{1}$01) and, because $\mathbf{b}$ was common to both reflections, $\mathbf{b}$ was found to be 1/3[11$\underline{2}$0]. Assuming that the growth is the same as the translation vector of the dislocation, these defects would be pure edge type in nature. The average threading dislocation density was also found along the plane normal to the growth direction. The dislocation density was found to be $\sim 8 \times 10^{10}$/cm^2.

The double-heterostructure sample was exposed to an Electron Cyclotron Resonance (ECR) plasma (500W of microwave power, 10 mTorr pressure) for 30 min at 200°C. The hole concentration in the p-GaN layer was reduced from 3×10^{17}cm^{-3} to $\sim 2 \times 10^{16}$cm^{-3} by this treatment, as measured by capacitance voltage (C-V) at 300K. Sections from this material were then annealed for 20 mins at temperatures from 500-900°C under an ambient of either N$_2$ or H$_2$ in a Heatpulse 410T furnace. Fig. II.2 shows the percentage of passivated Mg remaining after annealing at different temperatures in these two ambients. In the case of N$_2$ ambients the Mg-H complexes show a lower apparent thermal stability (by ~ 150°C) than with H$_2$ ambients. This has been reported previously for Si donors in InGaP and AlInP, and Be and Zn acceptors in InGaP and AlInP, respectively, and most likely is due to indiffusion of hydrogen from the H$_2$ ambients, causing a competition between passivation and reactivation. Therefore an inert atmosphere is clearly preferred for the post-growth reactivation anneal of p-GaN to avoid any ambiguity as to when the acceptors are completely active. Previous experimental results by Brandt et.al. and total energy calculations by Neugebauer and Van de Walle suggest that considerable diffusion of hydrogen in GaN might be expected at ≤ 600°C.

Other sections of the double-heterostructure material were implanted with ^{2}H$^+$ ions (50keV, 2×10^{15}cm^{-2}) through a SiN$_x$ cap in order to place the peak of the implant distribution within the p$^+$GaN layer. Some of these samples were annealed at 900°C for 20 min under N$_2$. As shown in the Secondary Ion Mass Spectrometry (SIMS) profiles of Fig. II.3, the ^{2}H diffuses out of the p$^+$GaN layer and piles-up in the defective InGaN layer, which we saw from the TEM results suffers from thermal degradation during growth of the p$^+$GaN. Note that there is still sufficient ^{2}H in the p$^+$GaN ($\sim 10^{19}$cm^{-3}) to passivate all of the acceptors present, but electrical measurements show that the p-doping level was at its maximum value of $\sim 3 \times 10^{17}$cm^{-3}. These results confirm that as in other III-V semiconductors, hydrogen can exist in a number of different states, including being bound at dopant atoms or in an electrically inactive form that is quite thermally stable. We expect that after annealing above 700°C all of the Mg-H complexes have dissociated, and the electrical measurements show that they have not reformed. In other
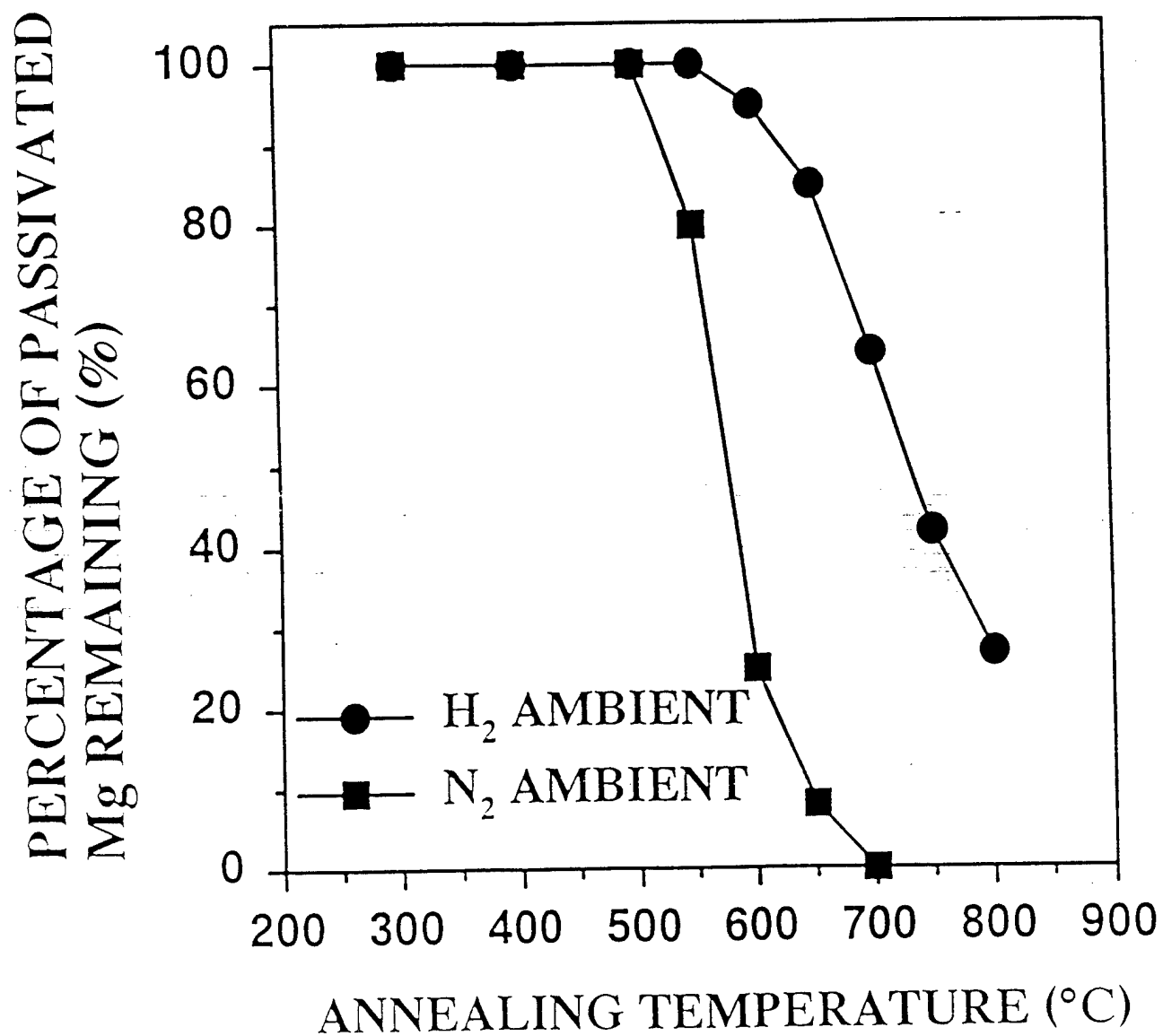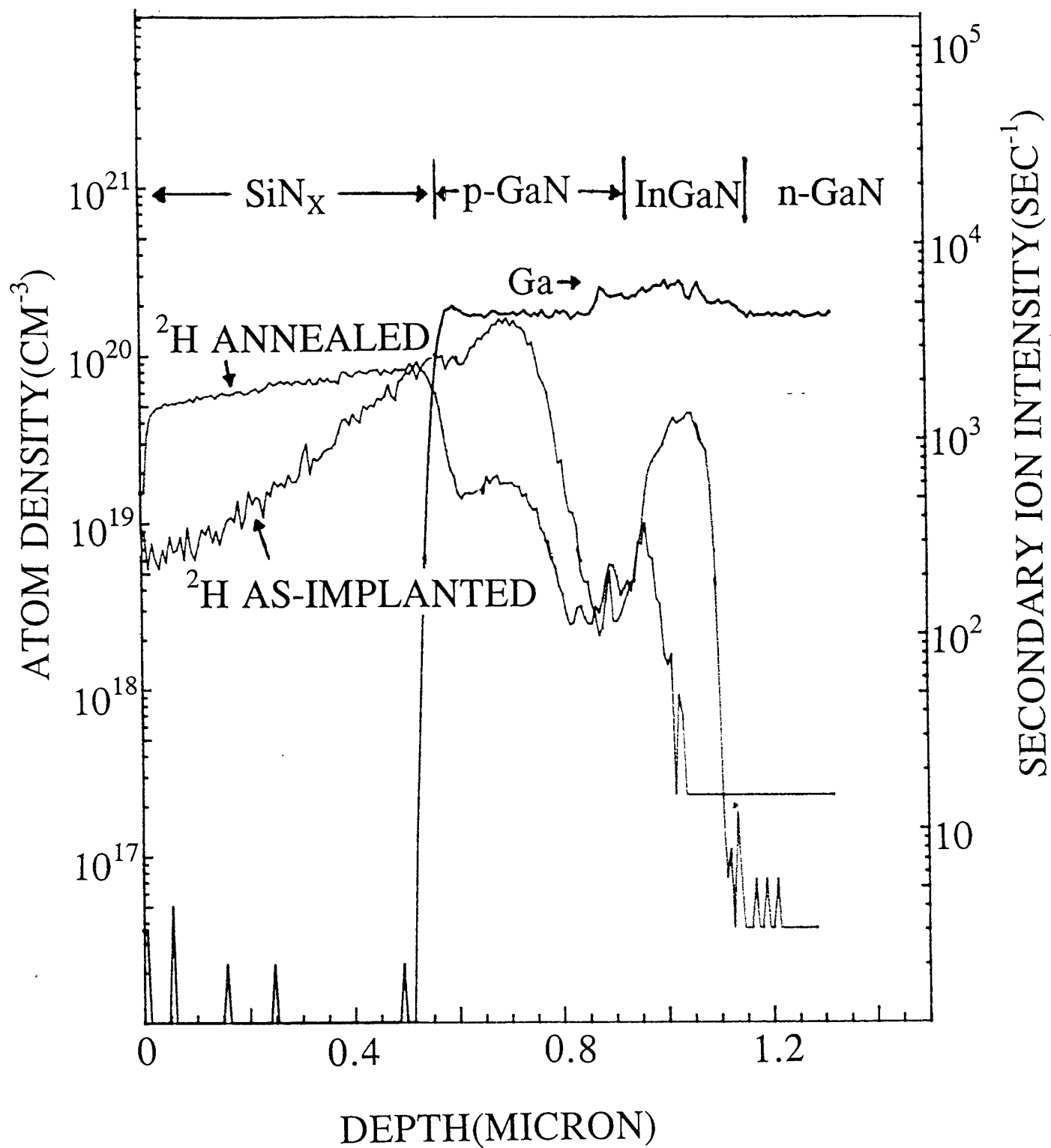
Fig. II.2.

Fig. II.3.

III-V's the hydrogen in p-type material is in a bond centered position forming a strong bond with a nearby N atom, leaving the acceptor 3-fold coordinated. Annealing breaks this bond and allows the hydrogen to make a short-range diffusion away from the acceptor, where it probably meets up with other hydrogen atoms, forming molecules or larger clusters that are relatively immobile and electrically inactive. This seems like a plausible explanation for the results of Figs. II.2 and 3, where the Mg electrical activity is restored by 700°C, but hydrogen is still present in the layer at 900°C. In material hydrogenated by implantation, there is almost certainly a contribution to the apparently high thermal stability by the hydrogen being trapped at residual implant damage as is evident by the fact that the ^{2}H profile retains a Pearson IV type distribution even after 900°C annealing. The other important point from Fig. II.3 is that as in other defective crystal systems hydrogen is attracted to regions of strain, in this case the InGaN sandwiched between the adjoining GaN layers.

In conclusion, the apparent thermal stability of hydrogen-passivated Mg acceptors in p-GaN is dependent on the annealing ambient, as it is in other compound semiconductors. While the acceptors are reactivated at ≤700°C for annealing under N_2, hydrogen remains in the material until much higher temperatures and can accumulate in defective regions of double-heterostructure samples grown on Al_2O_3. It will be interesting to compare the redistribution and thermal stability of hydrogen in homoepitaxial GaN in order to assess the role of the extended defects present in the currently available heteroepitaxial material.

b.   Inductively coupled plasma etching of GaN.

Inductively coupled plasma (ICP) etching offers an attractive alternative dry etching technique. The general belief is that ICP sources are easier to scale up than ECR sources, and are more economical in terms of cost and power requirements. ICP plasmas are formed in a dielectric vessel encircled by an inductive coil into which rf power is applied. A strong magnetic field is induced in the center of the chamber which generates a high-density plasma due to the circular region of the electric field that exists concentric to the coil. At low pressures (≤10 m Torr), the plasma diffuses from the generation region and drifts to the substrate at relatively low ion energy. Thus, ICP etching is expected to produce low damage while achieving high etch rates. Anisotropic profiles are obtained by superimposing a rf bias on the sample to independently control ion energy. In this letter, we report ICP etch results for GaN as a function of pressure, plasma chemistry, rf power and ICP power.

The GaN films etched in this study were grown by metalorganic chemical vapor deposition (MOCVD). The GaN film was approximately 1.8 μm thick and was grown on a c-plane sapphire substrate in a multiwafer rotating disk reactor at 1040°C with a 20 nm GaN buffer layer grown at 530°C. The ICP reactor used in this study was a load-locked Plasma-Therm SLR 770 etch system with the re-power supply operating at 2 MHz. Ion energies were provided by superimposing an rf bias (13.56 MHz) on the sample. Etch gases were introduced through an annular region at the top of the chamber. All samples were mounted using vacuum grease on an anodized Al carrier that was clamped to the cathode and cooled with He gas. Samples were patterned using AZ4330 photoresist. Etch rates were calculated from the depth of etched features measured with a Dektak stylus profilometer after the photoresist was removed with an acetone spray. Each sample was approximately 1 cm^2 and depth measurements were taken at a minimum of three positions. Error bars for the etch rates represent the standard
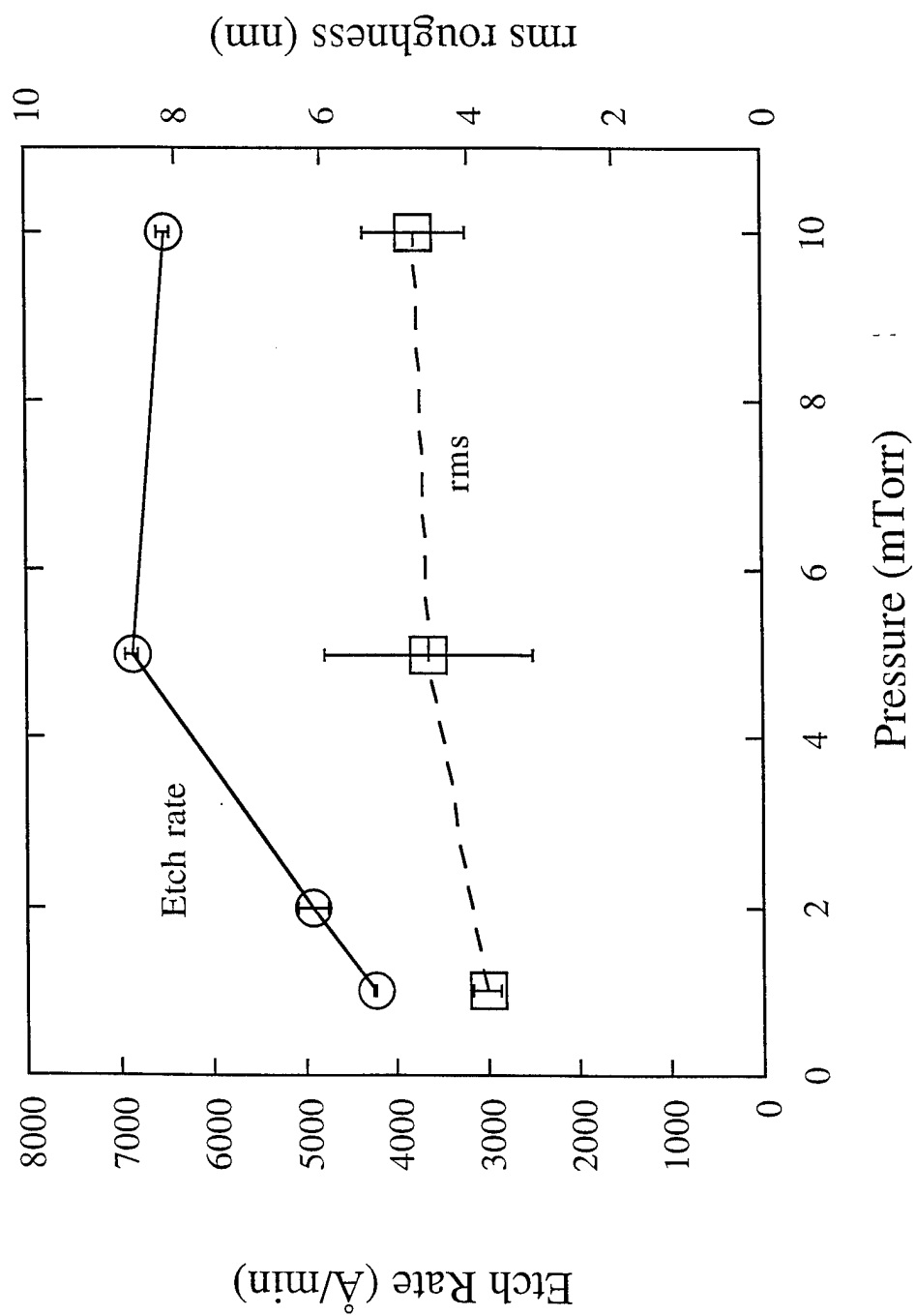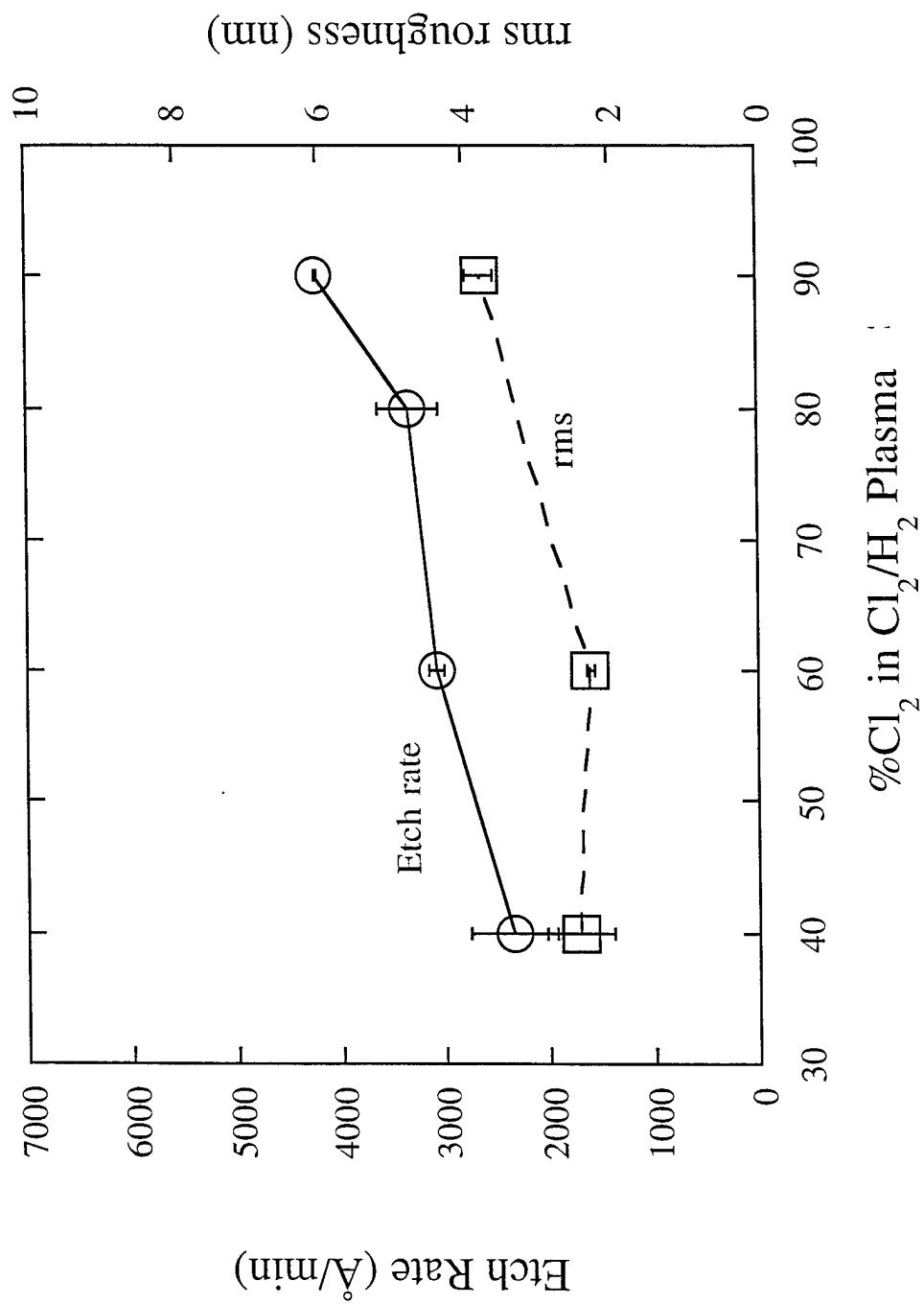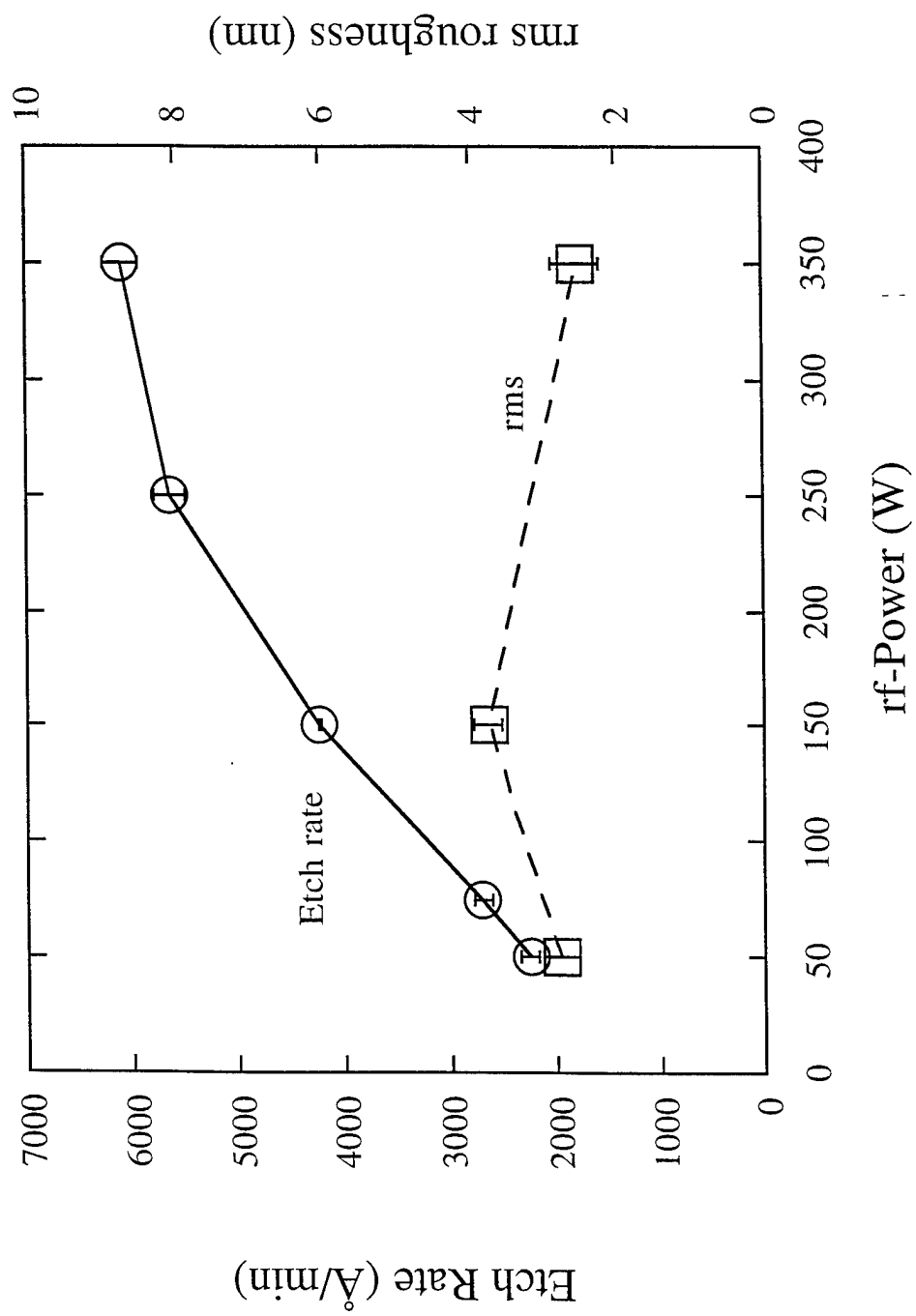
Fig. II.4.

Fig. II.5.

Fig. II.6.

rms roughness (nm)

rms
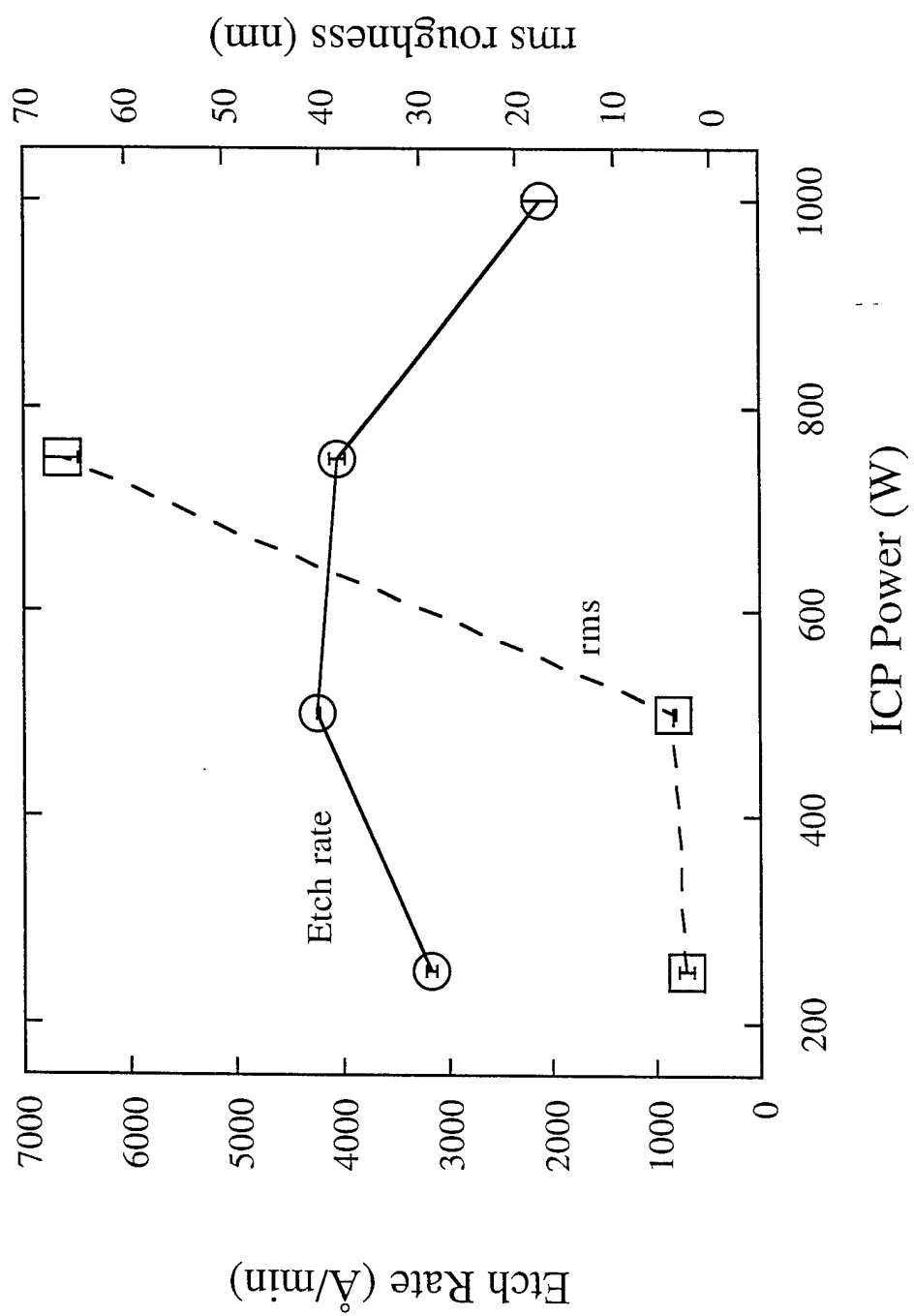
Etch rate
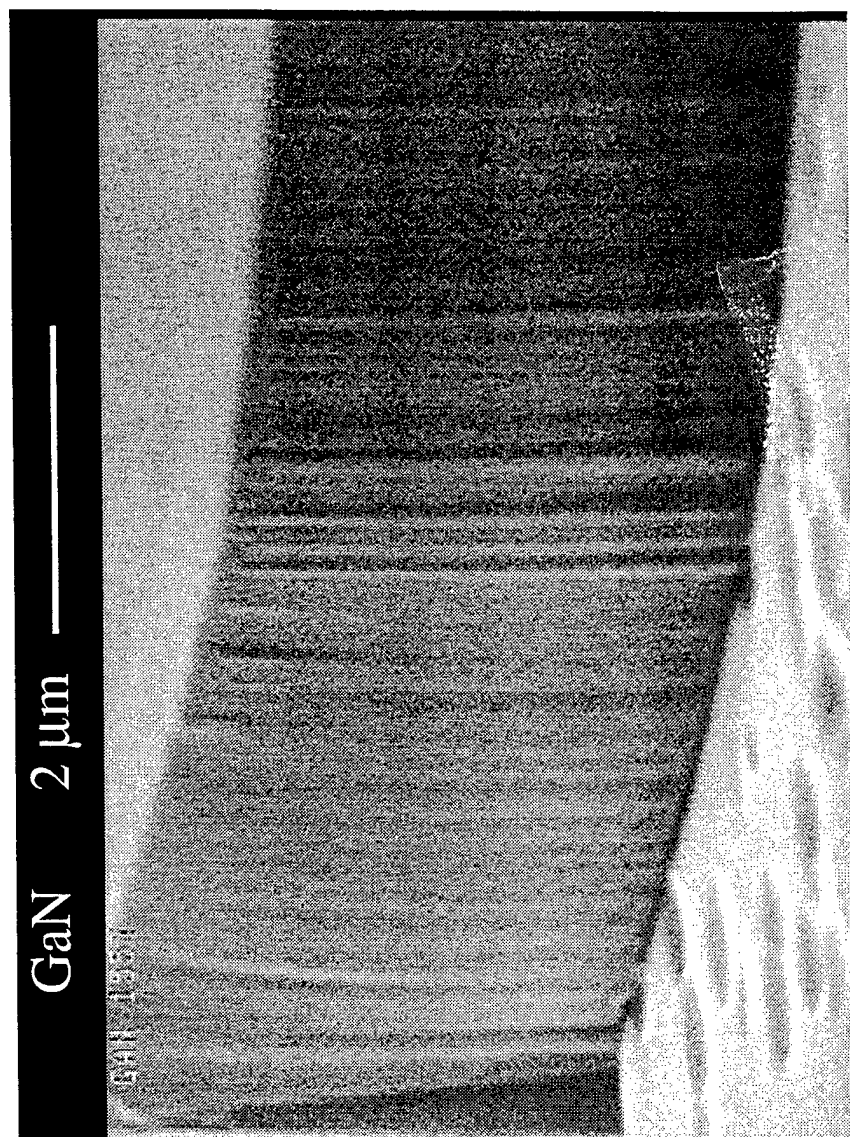
ICP Power (W)

Etch Rate (Å/min)

Fig. II.7.

Fig. II.8.

power, 22.5 sccm Cl$_2$, 2.5 sccm H$_2$, 5 sccm Ar, 25°C electrode temperature and 150 W rf power with a corresponding dc bias of -280±10 V. The GaN was overetched by approximately 15% at an etch rate of 6875Å/min with highly anisotropic, smooth sidewalls. The vertical striations observed by in the sidewall were due to striations in the photoresist mask which were transferred into the GaN feature during the etch. With optimization of the masking process, these etch parameters may yield profiles and sidewall smoothness enabling etched laser facets. The sapphire substrate was exposed during the overetch period and showed significant pitting possibly due to defects in the substrate.

In summary, ICP etching of GaN has been reported as a function of pressure, plasma chemistry, rf power and ICP power. GaN etch rates greater than 6875Å/min were measured, suggesting that high-density ICP is an excellent etch technique for nonselective etching of group-III nitrides and their alloys. The GaN rms roughness was smooth over a wide range of etch parameters, but appeared to be very sensitive to high-density plasma conditions (ICP power ≥750 W). Several ICP etch conditions showed direct application to the fabrication of group-III nitride etched laser facets.

(III)   Ohmic Contacts to p-GaN (Paul Holloway and Jeff Trexler)

Studies this quarter emphasized Pd/Au and Cr/Au contact metallizations which were compared to previous results from Ni/Au contacts to p-GaN. The GaN:Mg substrates used had a free hole concentration of 9.8x10^{16} cm^{-3}. All contacts were deposited by electron beam evaporation and consisted of 500A of Ni, Pd, or Cr followed by a 1000A Au capping layer. The contacts were heat treated up to 600C for up to 30 minutes in flowing N$_2$ and rapid thermally annealed (RTA) at 900C for 15 seconds. Current-voltage (I-V) measurements were taken after each anneal. Auger electron spectroscopy (AES) was performed on these samples following heat treatments to identify any interfacial reactions between the contact metals and the underlying GaN. Temperature dependent I-V measurements were taken for all the contact schemes to determine the dominant conduction mechanism.

The Pd/Au and Ni/Au as-deposited contacts were slightly rectifying with nearly linear I-V curves and low current transport. Upon heat treatment of the Ni/Au contacts the curves remained rectifying with a decreased potential offset at 400C. These changes in I-V are believed to be due to the break up of interfacial contamination. The Pd/Au contacts remained rectifying at all temperatures, with the lowest potential offset being observed following a 900C, 15 second RTA. The I-V curves for the Cr/Au contacts were rectifying as-deposited and remained so until a 900C, 15 second RTA. After this heat treatment, the I-V curve became linear indicating formation of an ohmic contact. The upper limit of the specific contact resistance of the Cr/Au contacts was estimated to be 4.3x10^{-1} Ωcm^2. The best I-V curves for each contact scheme are shown in Fig. III.1.

The purpose of the underlying Ni, Pd, or Cr for Ni in the contact schemes was to react with the underlying GaN and thus provide a greater opportunity for doping of the surface region of the GaN. AES depth profiles for the as-deposited Pd/Au contacts showed a planar interface between both the Pd:Au and Pd:GaN with no apparent interaction between the Pd/Au contact layer and the underlying p-GaN. After an RTA of 900C for 15 seconds, Pd had reacted with the Au capping layer to form a Au:Pd solid solution with slight incorporation and diffusion of Pd into GaN. (Fig. III.2). The Pd is thought to
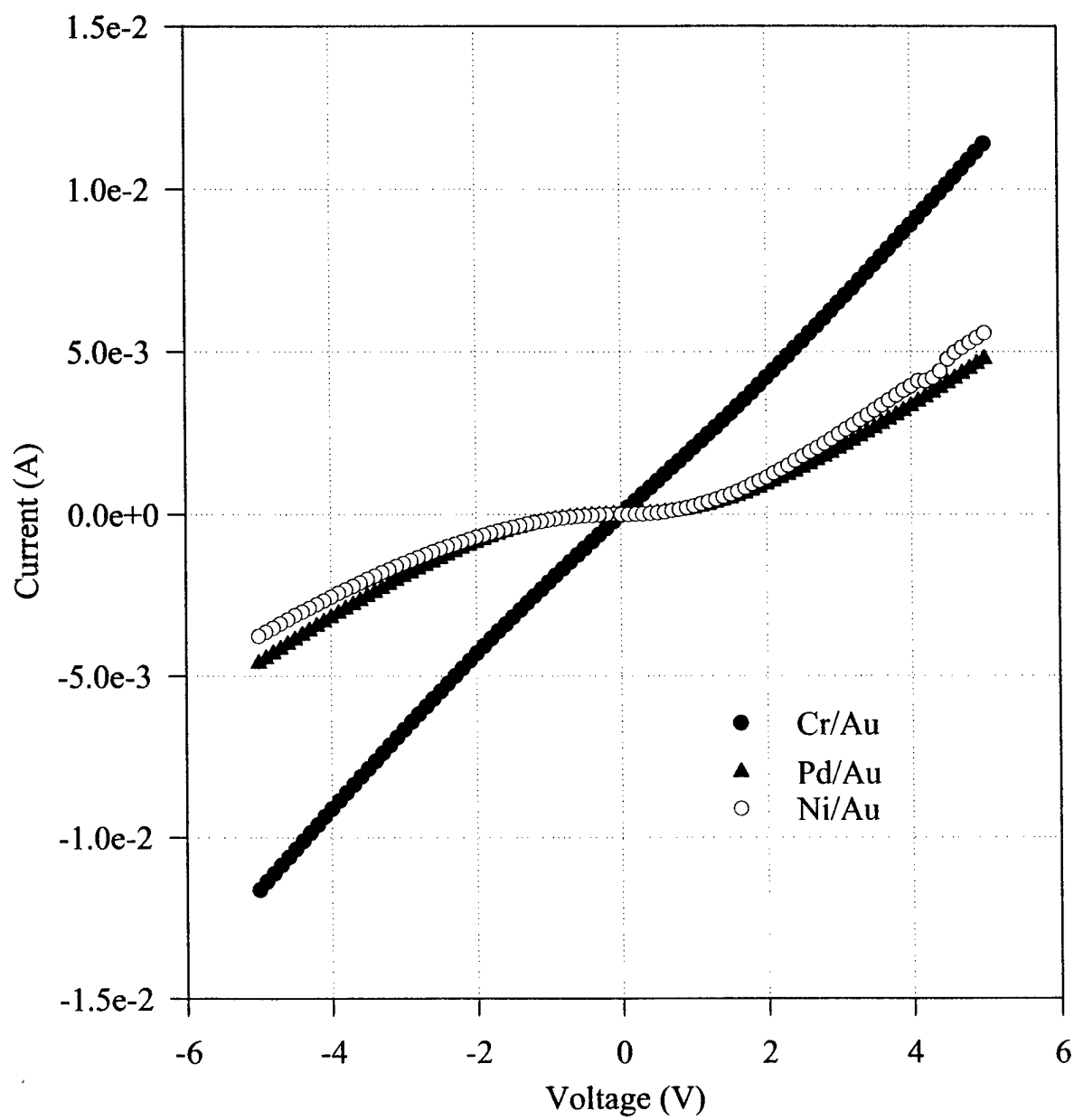
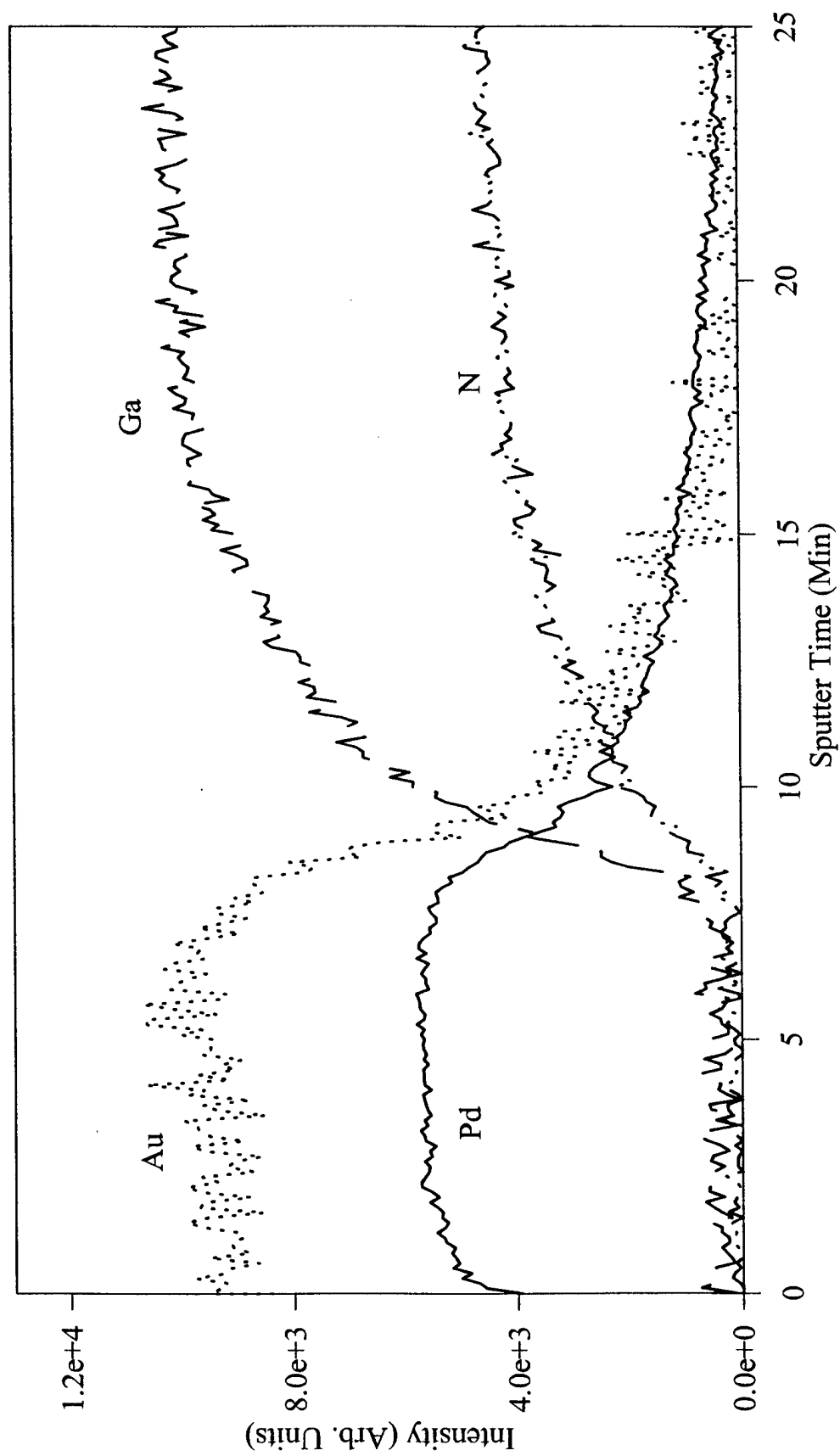**Fig. III.1.** I-V curves for Ni/Au, Pd/Au and Cr/Au

Fig. III.2. AES depth profile for Au/Pd/p-GaN. RTA 900°C, 15 seconds.

act as an acceptor, causing the near surface region to be more highly doped. For the Cr/Au contacts after an RTA of 900C for 15 seconds, the AES depth profile showed diffusion of Cr through the Au capping layer to the ambient/Au interface. There was some evidence of dissociation of GaN by Cr. An Au:Ga phase formed with excess N being incorporated into a Cr:N phase at the metal/semiconductor interface. (Fig. III.3) It is suggested that the Cr:N phase has a higher work function than the individual metals, reducing the potential offset at the interface.

Temperature dependent I-V data for the Ni/Au and Pd/Au contacts showed a large increase in current with increased temperature, indicative of thermionic emission. The conduction across the Cr/Au contacts was relatively stable over the temperature range investigated. In all cases, there appeared to be a change in conduction mechanism at about 2.5-3 eV. It appears that conduction above this value is dominated by a tunneling mechanisms (either thermionic field emission or field emission) while at voltages below 2.5 eV thermionic emission is dominating the conduction. Work on determining the conduction mechanism(s) for these three contact schemes will continue.

(IV)   Microstructures of GaN Film and LiGaO$_2$ (Kevin Jones and Jing Hong Li)

Research work is being continued on microstructural characterization of GaN films grown by MOCVD on LiGaO$_2$ since the substrate is one of key factors to determine the crystalline quality of the grown GaN film, especially the surface microstructure of the substrate at initial stage of the film growth.

Fig. IV.1 shows a cross-section TEM micrograph of a rather high quality GaN film. It reveals that there still are high density of threading dislocations and stacking faults as observed previously. In addition to these defects, another type of defects has been identified as inversion domain boundaries (IDBs, marked as "ID"), where the GaN structure is inverted or displaced along the c-axis due to nucleation of the opposite phase at the substrate, as shown in Fig. IV.2. Fig. IV.2 (a) is bright field TEM micrograph, while Figs. IV.2 (b) and (c) are dark field TEM micrographs imaged with g=0002 and g=0002 near the [1120] zone axis of GaN, respectively. These columinar IDBs are similar with that found by others in GaN films grown by molecular beam epitaxy (MBE). It was believed that IDBs are a significant source of defects in GaN grown by any technique (*Romano etc. 1996*). Fig. IV.3 shows HRTEM image of the GaN/LiGaO$_2$ interface. Some islands are observed at the interface, indicating that an interfacial chemical reaction occurred during the GaN growth. And there was still a nano-crystalline or amorphous interlayer between the GaN and the LiGaO$_2$. This speculation of interfacial reaction is confirmed by a preliminary compositional study using Secondary Neutrals Mass Spectroscopy (SNMS) (*Kryliouk etc., 1996*). The SNMS result showed that the interlayer is rich in Li. So it is possible that another Li-riched phase such as Li$_5$GaO$_4$ could be formed at the GaN/LiGaO$_2$ during the film growth. Also our result about the possible interface reaction is consistent with SIMS result from *Kryliouk* (1996) which shows that Li has diffused into the GaN near the GaN/LiGaO$_2$ interface. Fig. IV.4 shows another HRTEM image of the GaN film about 0.1μm from the GaN/LiGaO$_2$ interface. It was found that the grown GaN film contains both hexagonal wurtzite structure (marked as "WS") and cubic zinc-blende structure (marked as "ZS"). Between these two structures there is a stacking fault. It is assumed that this microstructure is caused by the change of temperature gradient between the grown GaN film
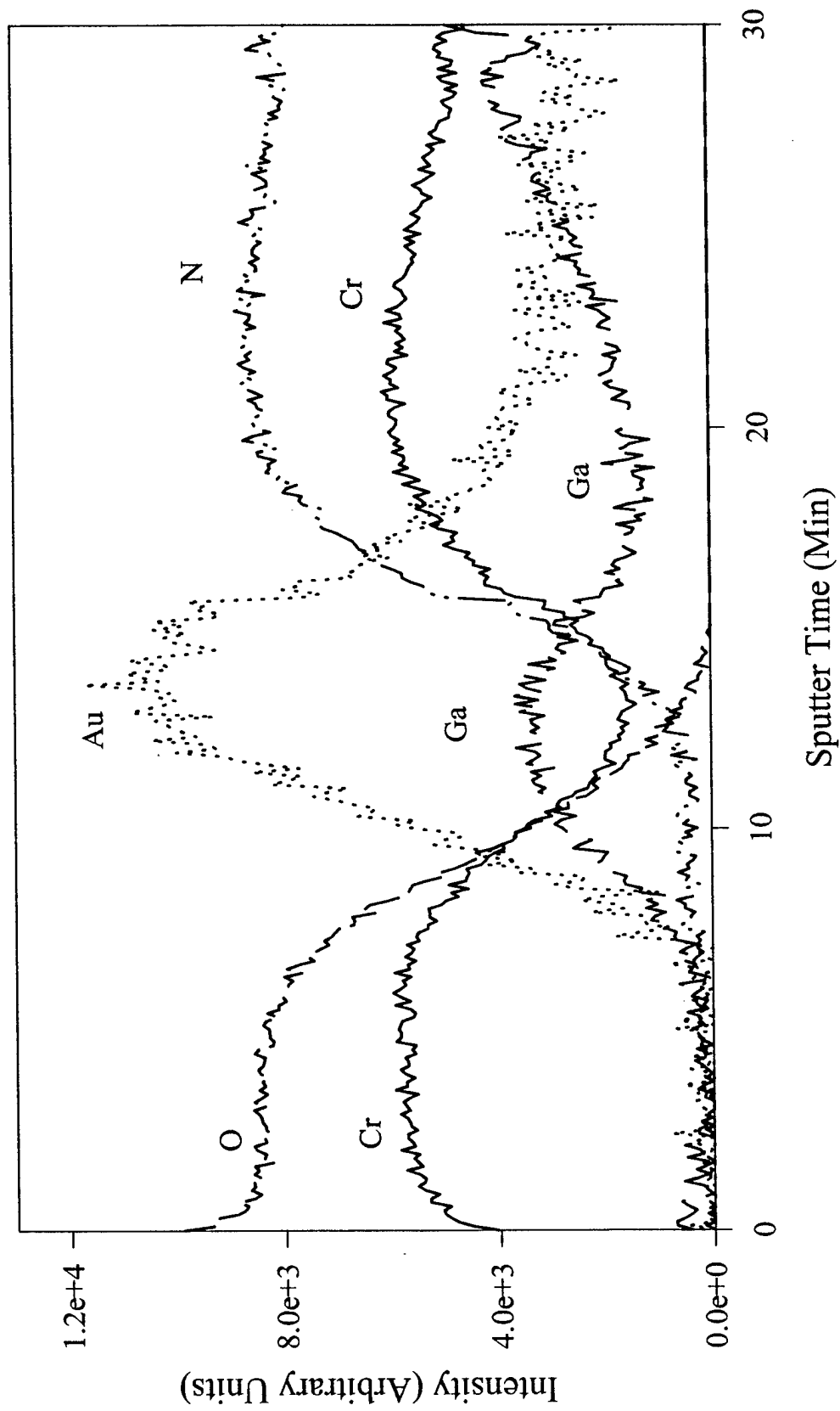
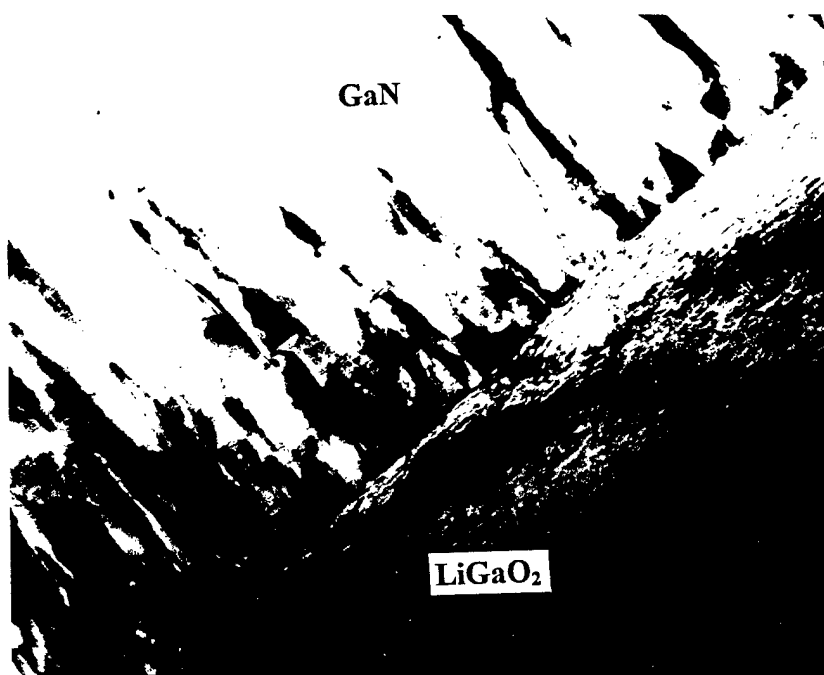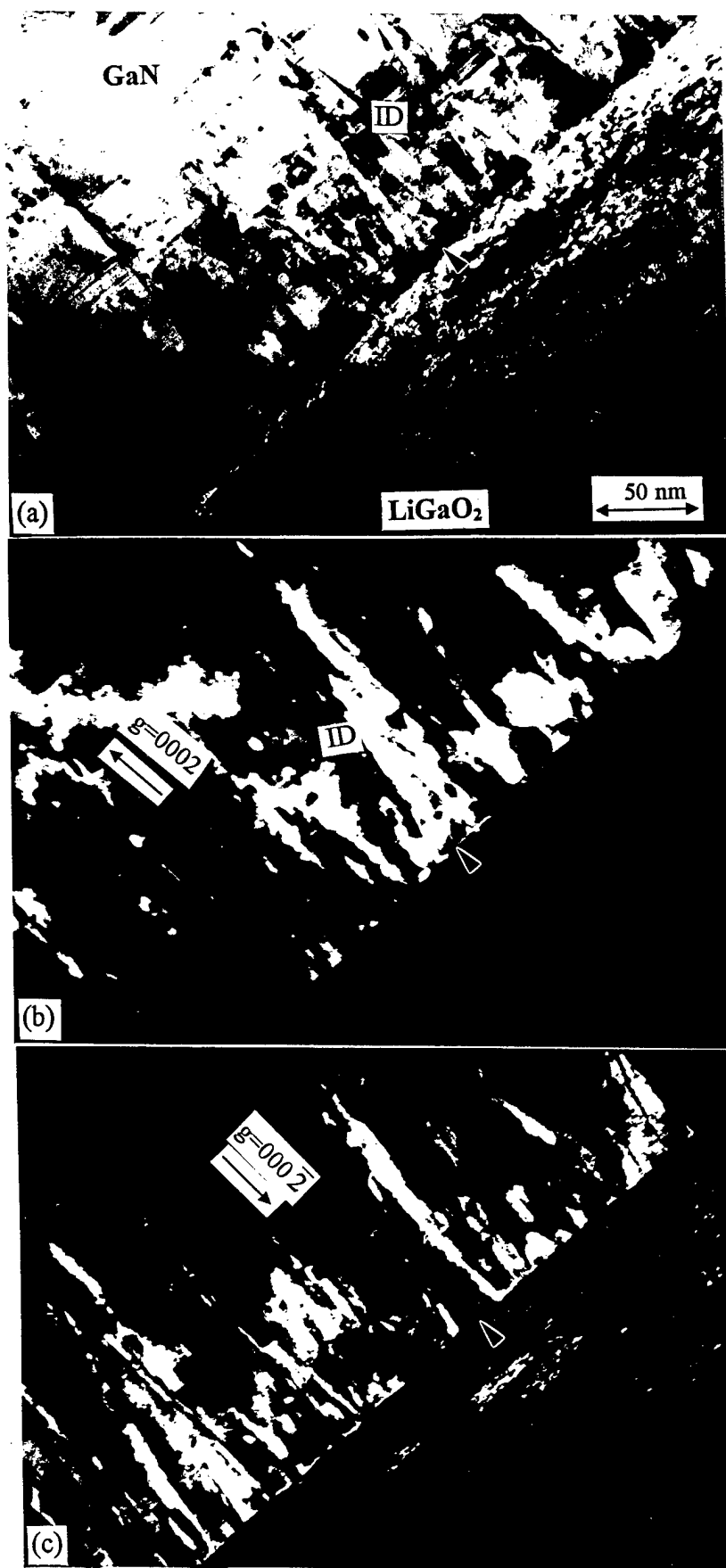**Fig. III.3.** AES depth profile for Au/Cr/p-GaN, RTA 900°C, 15 seconds.
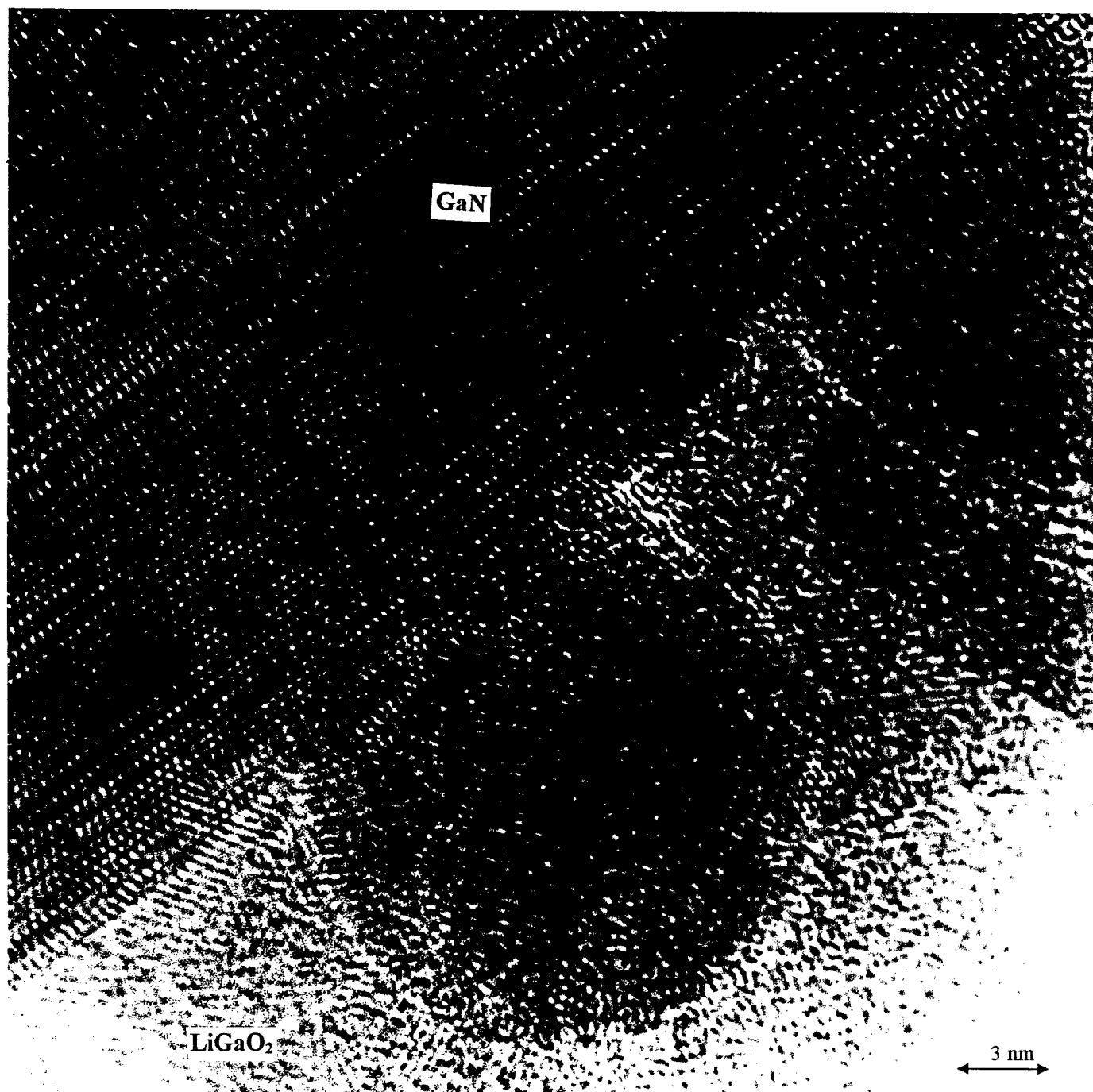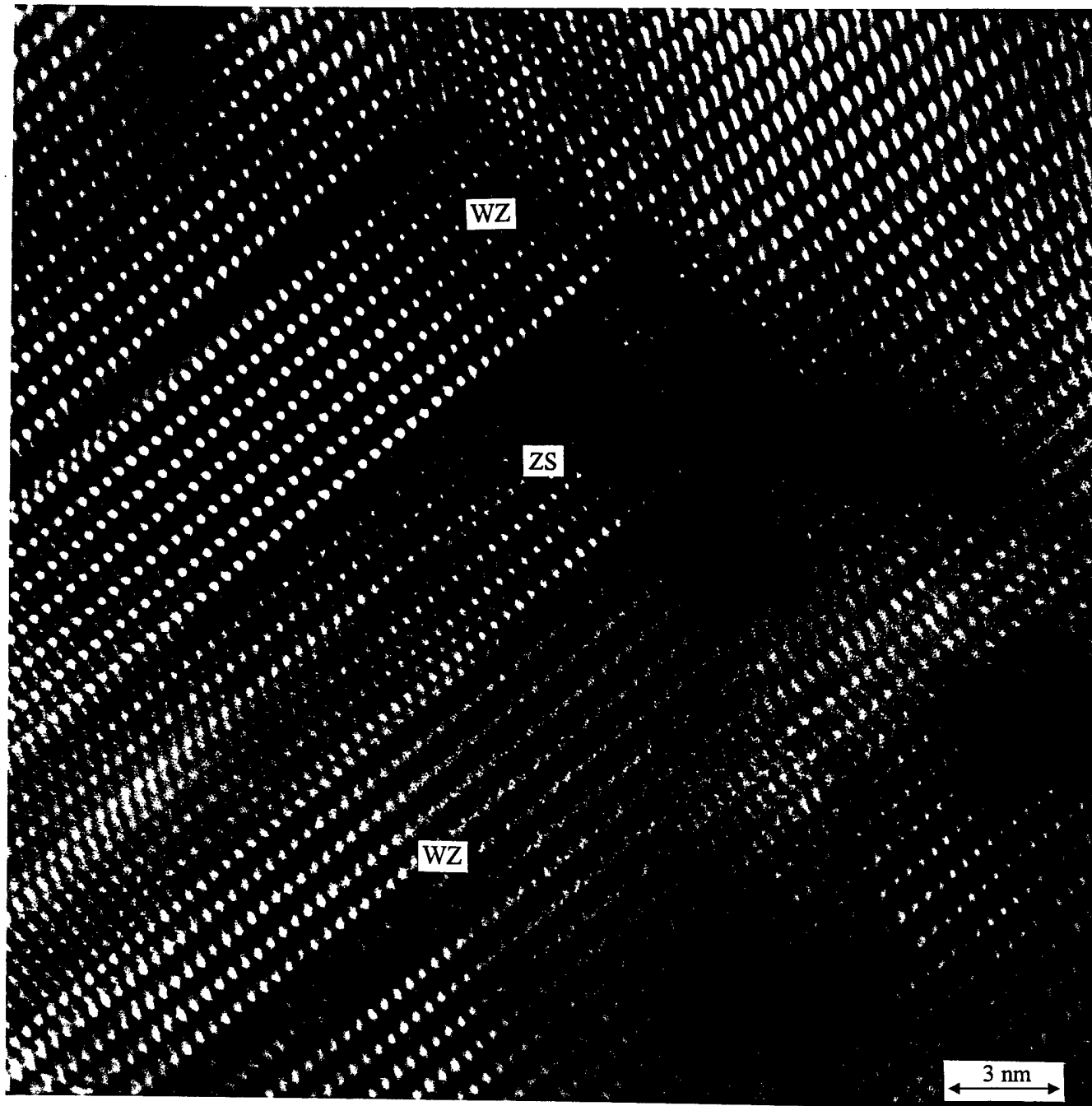
Fig. IV.1.

Fig. IV.2.

Fig. IV.3.

Fig. IV.4.

and the LiGaO$_2$ substrate during the film growth. The difference between the wurtzite and cubic zinc-blende crystal structures lies the stacking sequence of bilayers of the Ga and N atoms. The former one has an ABABAB... sequence along its [0001] direction, and the later one has an ABCABC... stacking sequence along its [111] direction. So when the ideal stacking sequence is broken, a stacking fault is introduction, as illustrated by Fig. IV.5.

Since the surface microstructure of the LiGaO$_2$ is one of key factors to control crystalline quality of the grown GaN film, it is necessary to study the initial surface microstructure before film growth. Fig. IV.6 is a cross-sectional HRTEM image of surface microstructure of the LiGaO$_2$. It shows that the surface of the LiGaO$_2$ is not atomic flat and there is a 20 nm deep disordered region. Dark contrast indicated that residual strains remain in the surface region after mechanical and chemical polishing the LiGaO$_2$ single crystal. Down to the 20 nm disordered region, the LiGaO$_2$ has a perfect crystalline structure with few defects. The observed surface damage region may be caused by mechanical cutting and chemical polighing. Chemical polishing using inorganic acids such as HC1 did not remove all the surface damage region caused by mechanical cutting. The disordered region may also be caused by anisotropic chemical polishing. As LiGaO$_2$ and GaN have a very close lattice mismatch (~0.1%), the dislocation density is expected low compared with other substrates. But, as we report before, the dislocation density is still quite high. The observed poor surface of the LiGaO$_2$ is presumably one reason responsible for the observed high dislocation density in the grown GaN film. In a recent study on LiGaO$_2$ by *Limpijumnong* etc. (1996), it is found that Li-O has a weaker bond strength than Ga-O in LiGaO$_2$. So the Li-O bonding in the surface region could be firstly broken by the mechanical cutting or chemical polishing, leading to the formation of the nano-crystalline or amorphous disordered interlayer as the above observed by HRTEM. Further work is being continued using EELS and the nitrogen pre-treated LiGaO$_2$ will be carried out to improve the crystalline quality of GaN.

In summary, electron microscopy study is being continued in the GaN/LiGaO$_2$. Inversion domain boundaries has been identified in the GaN film. Interfacial reaction between the GaN and LiGaO$_2$ has been observed. Both hexagonal wurtzite and cubic zinc-blende structures have been found in the grown GaN film. A disordered damage region with a depth of 20 nm has been found by HRTEM at the surface of the LiGaO$_2$ will be carried out to improve the crystalline quality of GaN.

(V)   CdZnSe Quntum Well (QW) Diode Laser Material (Peter Zory)

CdZnSe diode laser material received from Michael Haase at 3M was processed and fabricated into a number of diode lasers with 100 micron wide stripes. Their lasing wavelength was measured as a function of laser length L and the data compared to predictions made using the II-VI laser model we have been developing. As discussed previously, the goal of this work is to establish the importance of Coulomb enhancement (CE) and other many-body effects in predicting the performance CdZnSe QW lasers. The measured shift in lasing wavelength over the range of cavity lengths measured is in good agreement with the model provided carrier scattering (CS), bandgap renormalization (BGR) and CE are included in the computations. This work will be reported on at the SPIE Photonics West Conference in San Jose in February.
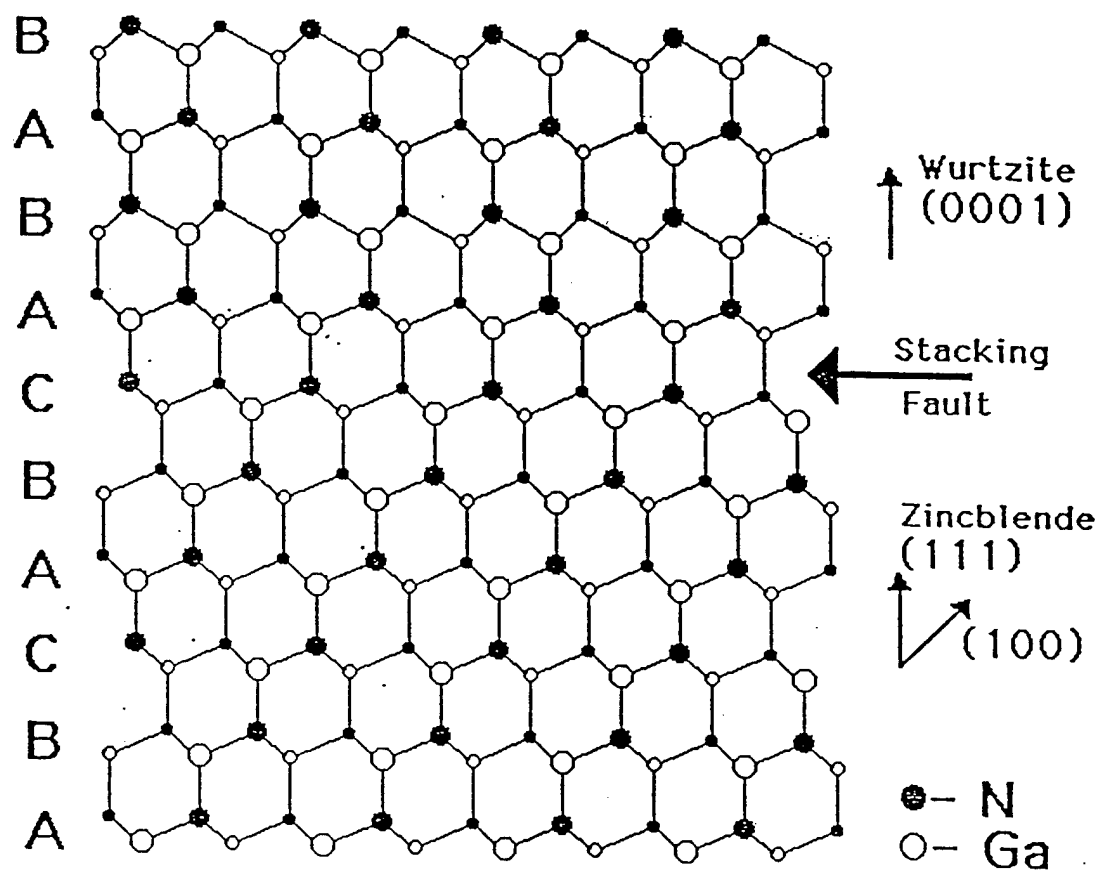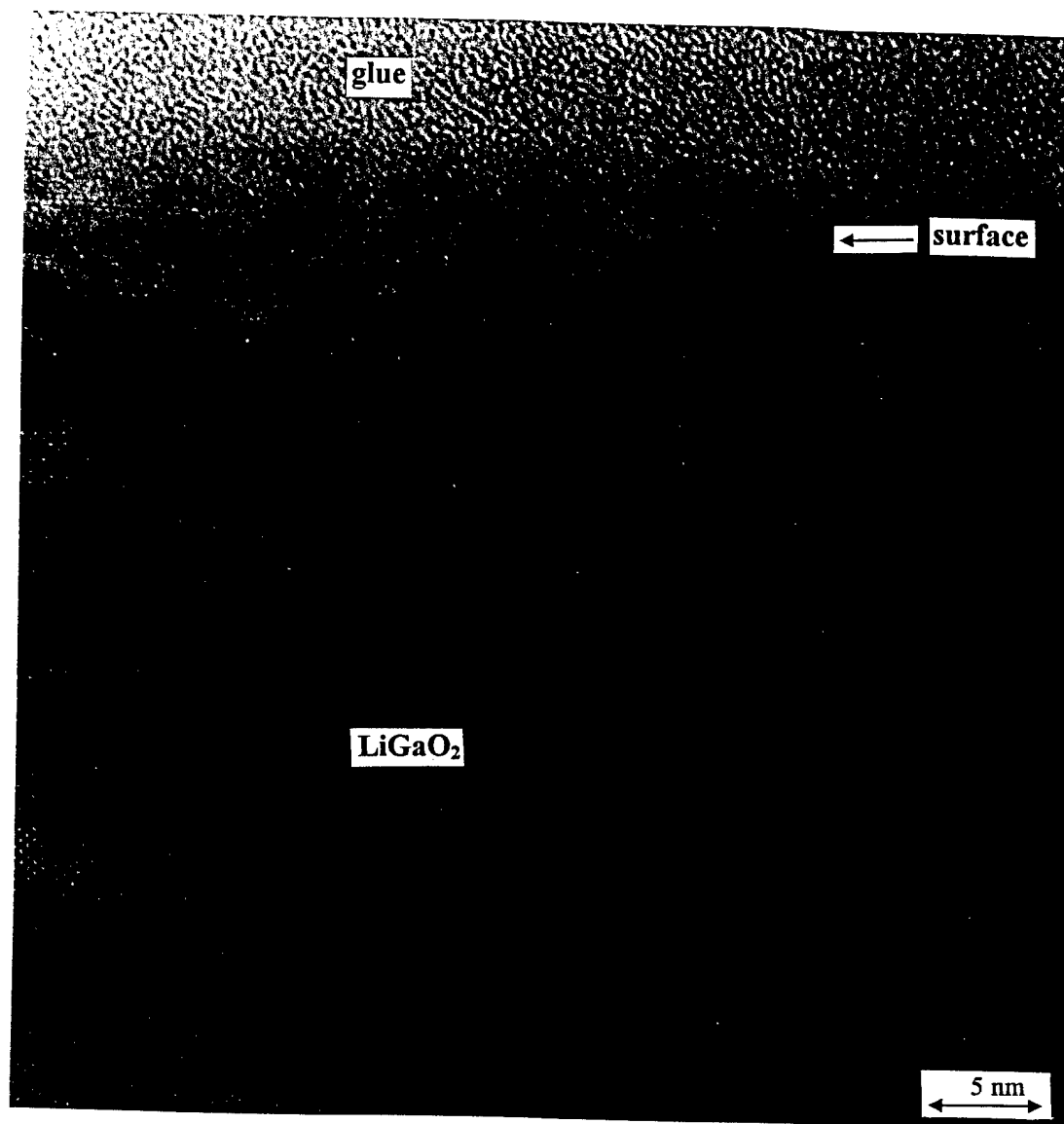
Fig. IV.5.

Fig. IV.6.

As an additional check on the model, InGaAs QW / GaAs, 100 micron stripe lasers with operating wavelengths in the vicinity of 950 nm were also fabricated, characterized and compared to the model. Based on published work, it was expected that CE should not be important in such lasers. We found however that the optical gain and spontaneous emission spectra are changed substantially by CE and that one needs CE if one is to successfully model the dependence of lasing wavelength on L. The work on InGaAs lasers has been written up and submitted to the IEEE Journal of Quantum Electronics for publication in the Special Issue on Semiconductor Lasers.

The CdZnSe lasers described above were operated at the 200 mW pulsed level and demonstrated to Air Force personnel from Phillips Lab in Albuquerque, NM (30 Oct 96). They are interested in green diode lasers for various defense applications.

InGaN QW LED Material

Additional work was done on the electrochemical technique for etching InGaN QW LED material described previously and a paper prepared for publication.

(VI)   Optical and Electrical Characterization of ZnSe (Joe Simmons)

We have spent the past quarter re-examining the mobility of carriers in ZnSe and have developed a new model for the static screening effect of ionized impurities in n-doped ZnSe. The approach develops a self-consistent screening theory derived under the Born Approximation. Compensation is taken into account and becomes a key parameter in the calculation of the screening efect. Comparisons with literature data are presented. We are working on genrealization of the model to other semiconductors for which mobility data is available. This work is conducted in conjunction with Drs. Stanton and Sanders and Mr. J. Li from Physics Department.

(VII)   Visible Light Emitting Materials and Devices (G.F. Neumark)

We continued working on the problem of non-equilibrium doping during MBE growth of ZnSe:N. We have concluded that the dopant concentration is limited mostly by solubility. Solubility is low under Se rich conditions, which are conventionally used for good growth.

PhD. Dissertation:

- "Impact of the Growth Kinetics on Deep Level Defect Production in GaN Films Grown by MBE," Hsing-Long (Bruce) Liu, Ph.D., Dec. 1996.

References:

- H. Z. Xiao, N-E. Lee, R. C. Powell, Z. Ma, L. J. Chou, L. H. Allen, J. E. Greene and A. Rockett, J. Appl. Phys., **76** (12), 8195 (1994).
- D. J. Smith, D. Chandraskhar, B. Sverdlov, A. Botchkarev, A. Salvador and H. Morkoc, Appl. Phys. Lett., **67** (13), 1830 (1995).
- F. R. Chien, X. J. Ning, S. Stemmer, P. Pirouz, M. D. Bremser and R. F. Davis, Appl. Phys. Lett., **68** (19), 2678 (1996).
- F. A. Ponce, B. S. Krusor, J. S. Major, Jr., W. E. Plano and D. F. Welch, Appl. Phys. Lett., **67**(3), 410 (1995).
- "MOCVD Growth of GaN Films on Lattice-Matched Oxide Substrates," O. Kryliouk, T.W. Dann, T.J. Anderson, H.P. Maruska, L. Zhu, J. Daly, M. Lin, P. Norris, B. Chai, D. Kisker, J.H. Li and K.S. Jones, 1996 MRS Proceedings: Gallium Nitrides and Related Materials, accepted.
- "Bond Structure and Cation Ordering in LiGaO$_2$," Limpijumnong, W.R.L. Lambrech, B. Segall and K. Kim, 1996 MRS Proceedings: Gallium Nitrides and Related Materials, accepted.
- L.T. Romano, J.E. Northrup, M.A. O'Keefe, (1996) Appl. Phys. Lett. 69 (16), 2394-2396.

Publications:

- "ICl/Ar ECR Plasma Etching of III-V Nitrides," C. Vartuli, S. Pearton, J. Lee, J. Hong, J.D. MacKenzie, C.R. Abernathy and R.J. Shul, Appl. Phys. Lett. 69, 1426 (1996).
- "Reactivation of Acceptors and Trapping of Hydrogen in GaN/InGaN Double Heterostructures," S.J. Pearton, S. Bendi, K.S. Jones, V. Krishnamoorthy, R.G. Wilson, F. Ren, R. Karlicek and R.A. Stall, Appl. Phys. Lett. 69, 1879 (1996).
- "Er doping of AlN During Growth by MOMBE," J.D. MacKenzie, C.R. Abernathy, U. Hommerich, X. Wu, R.N. Schwartz, R.G. Wilson and J.M. Zavada, Appl. Phys. Lett. 69, 2083 (1996).
- "Damage to Epitaxial GaN Layers by Ion Implantation," H. Tan, J.S. Williams, J. Zou, D. Cockayne, S.J. Pearton and R. Stall, Appl. Phys. Lett. 69, 2364 (1996).
- "Wet and Dry Etching of LiGaO$_2$ and LiAlO$_2$," J. Lee, S. Pearton, C. Abernathy, J. Zavada and B. Choi, J. Electrochem. Soc. 143, L169 (1996).
- "Electrical Transport in p-GaN, n-InN and n-InGaN," W. Geerts, J. MacKenzie, C. Abernathy, S. Pearton and T. Schmeidel, Solid State Electron. 39, 1289 (1996).
- "Cl$_2$/Ar and CH$_4$/H$_2$/Ar Dry Etching of III-V Nitrides," C. Vartuli, J. MacKenzie, J. Lee, C. Abernathy, S. Pearton and R. Shul, J. Appl. Phys. 80, 3705 (1996).
- "High Density Etching of Group III Nitrides Ternary Films," R. Shul, A. Howard, S. Pearton, C. Abernathy and C. Vartuli, J. Electrochem. Soc. 143, 3285 (1996).

- "Selective Dry Etching of III-V Nitrides in Cl_2/Ar, CH_4/H_2/Ar, ICl/Ar and IBr/Ar," C. Vartuli, S. Pearton, J. MacKenzie, C. Abernathy and R. Shul, J. Electrochem. Soc. 143, L246 (1996).
- "Wet Chemical Etching of AlN and InAlN n KOH Solutions," C. Vartuli, S. Pearton, J. Lee, C. Abernathy, J. MacKenzie, J. Zolper, R. Shul and F. Ren, J. Electrochem. Soc. 143, 3681 (1996).
- "Low Energy Electron-enhanced Etching of GaN/Si in Hydrogen dc Plasma," H. Gillis, D. Choutov, K. Martin, S. Pearton and C. Abernathy, J. Electrochem. Soc. 143, L251 (1996).
- "High Ion Density Dry Etching of Compound Semiconductors," S. Pearton, Mat. Sci. Eng. B40, 101 (1996).
- "Plasma Damage Effects in InAlN FETs," F. Ren, J. Lothian, J. MacKenzie, C. Abernathy, C. Vartuli, S. Pearton and R. Wilson, Solid. State Electron. 39, 1747 (1996).
- C. Kothandaraman, I. Kuskovsky, G.F. Neumark, R.M. Park, "Time-resolved luminescence of heavily nitrogen doped ZnSe", Appl. Phys. Lett., 69, (1996), 1.
- I. Kuskovsky, G.F. Neumark, "Doping and non-equilibrium during low-temperature growth (application to MBE)", ISCS-23 Proc., in press.
- C. Kothandaraman, G.F. Neumark, and J.A. Kash, "Temperature evolution of excitonic luminescence in nitrogen doped zinc selenide", Appl. Phys. Lett., submitted.

Presentations:
- "Direct Generation of Short-Wavelength Radiation by Wide-Bandgap Semiconductor Diode Lasers: A Review of Materials Developments," R.M. Park, Optical Society of American Annual Meeting, Rochester, NY, Oct. 20-25, 1996.
- "Critical Issues of III-V Compound Semiconductor Processing," S.J. Pearton, Invited presentation at 25th SOTAPOCS Symp., ECS Meeting, San Antonio, Oct. 1996.
- "Plasma Induced Damage in GaN," R. Shul, S. Pearton, J. Lee, R. Kurlecek and C. Constantine, Invited presentation at 25th SOTAPOCS Symp., ECS Meeting, San Antonio, Oct. 1996.
- "The Role of AlN Encapsulation of GaN During Implantation Activation Annealing," J. Zolper, S. Pearton, J. Lee, C. Vartuli and R. Stall, Invited presentation at 25th SOTAPOCS Symp., ECS Meeting, San Antonio, Oct. 1996.
- "Structural and Chemical Investigation of WSi_x Ohmic Contacts on n^+GaN," M. Cole, F. Ren and S.J. Pearton, 25th SOTAPOCS Symp., ECS Meeting, San Antonio, Oct. 1996.
- "Effects of Dry Etching on III-Nitride Surface Properties," F. Ren, S. Pearton, C. Abernathy, C. Vartuli, R. Kurlecek, J. MacKenzie and R. Wilson, 25th SOTAPOCS Symp., ECS Meeting, San Antonio, Oct. 1996.
- "RTP of III-Nitrides," J. Hong, C. Vartuli, S. Pearton, C. Abernathy and J.C. Zolper, 43rd Nat. AVS Symp., Philadelphia, Oct. 1996.
- "Low Energy Electron Enhanced Etching of III-N Materials in H_2/Cl_2 dc Plasma," H. Gillis, D. Choutov, S. Pearton and C. Abernathy, 43rd Nat. AVS Symp., Philadelphia, Oct. 1996.

- "Comparison of Ohmic Metallization Schemes for InGaAlN," C. Vartuli, F. Ren, C. Abernathy, S. Pearton and R. Shul, 43rd Nat. AVS Symp., Philadelphia, Oct. 1996.
- "Zn^0 as a substrate for GaN," J. MacKenzie, C. Abernathy, S. Pearton, P. Holloway, B. Choi and R. Linares, 43rd Nat. AVS Symp., Philadelphia, Oct. 1996.
- "Plasma Etching of III-Nitrides in ICl and IBr," C. Vartuli, J. Lee, J. MacKenzie, C. Abernathy, S.J. Pearton and R.J. Shul, 43rd Nat. AVS Symp., Philadelphia, Oct. 1996.
- "Comparison of Ni/Au, Pd/Au, and Cr/Au Metallizations for Ohmic Contacts to p-GaN," J.T. Trexler, S.J. Pearton, P.H. Holloway, M.G. Mier, K.R. Evans, and R.F. Karlicek. Presented at the MRS 1996 Fall Meeting, December 2-6, 1996, Boston, MA. To be published in Mat. Res. Soc. Symp. Proc. Symposium N, III-V Nitrides.
- I. Kuskovsky, G.F. Neumark, "Doping and non-equilibrium during low-temperature growth (application to MBE)",ISCS-23, St. Petersburg, Russia.
- I. Kuskovsky, G.F. Neumark, V.N. Bondarev, and P.V. Pikhitsa, "Application of Fluctuation Theory to the Time-Resolved Luminescence from Heavily Doped Semiconductors", to be presented, APS, March' 97.
- G.F. Neumark, I. Kuskovsky, "Doping Problems in Wide Bangap Materials Revisited", to be presented, APS, March' 97.

Post Doctoral Associates:

    Jing Hong Li with Dr. Jones

    Olga Kryliouk with Dr. Anderson

Graduate Students Supported:

    Bruce Liu with Dr. Park

    George Kim with Dr. Park

    Brent Gila with Dr. Park

    Jin Hong with Dr. Pearton

    K.N. Lee with Dr. Abernathy

    Jeff Trexler with Dr. Holloway

    Joe Thomes with Dr. Holloway

    Todd Dann with Dr. Anderson

    Jeff Hsu with Dr. Zory

    Jason O with Dr. Zory

    John Yoon with Dr. Zory

    Igor Kuskovsky with Dr. Neumark